

Sediment-Water Interactions

Ellen L. Petticrew

This chapter addresses sediment-water interactions and comprises five sections, with the papers investigating a variety of chemical, physical and biological processes that influence the behavior of sediments in natural waters. The approaches used range from small-scale laboratory studies that attempt to simulate natural conditions, to in-stream manipulation of sediments, to seasonal studies of in-stream sediments collected in a variety of environmental conditions. The goal of this type of work, as indicated in most of the sections, is to improve our knowledge of the processes regulating sediment-water interactions so as to allow the most suitable approach to managing the aquatic environment, whether it be for maintaining benthic habitats or decision-making regarding the removal of contaminated sediments.

The initial chapter addresses issues and methods for source identification of organic matter in riverine suspended sediments as it has been shown to have a significant influence on the morphology and the transport behavior of flocculated fine sediments. The values of both C:N ratios and stable isotopes of C and N allow seasonal differentiation of suspended organic matter in a northern, temperate productive stream. While this paper deals with the particulate organic matter moving as aggregated or flocculated sediments in a natural stream system, Sect. 6.2 presents a laboratory study investigating the role of various factors which regulate fine sediment aggregation and stability. Ionic concentration is the dominant factor associated with aggregation in this experimental system. Increased levels of heavy metal adsorption onto natural riverine sediment, as opposed to kaolin clay, suggests a concern regarding the storage of heavily polluted natural sediments in environments which promote aggregation and therefore sedimentation. Section 6.3 evaluates the influence of variable, natural aquatic levels of dissolved organic matter (DOM), which is also a factor that can influence sediment-water interactions, on the sorption and desorption kinetics of select organic contaminants. This work was undertaken in order to better inform knowledge of issues related to contaminant remobilization from polluted sediments. While the experimental range of DOM was not found to be significant, the hydrodynamic conditions and contaminant contact time were found to influence desorption. Section 6.4 combines meso-scale field and laboratory experiments to address resuspension and transport behavior of channel-stored riverine sediment. The results of the field experiment confirm the natural heterogeneity of riverine surficial fine sediments associated with the 'fluffy layer' on the channel bed that is not well represented in laboratory experiments. This suggests that sediment-water laboratory experiments can underestimate pollutant mobility in natural systems. Section 6.5 presents results of an experiment using a benthic cham-

ber to assess metal mobility associated with different levels of critical shear stress, which modifies both the resuspended loads and the physical form (aggregated versus dispersed) of the sediments. The implication of eroding sediments to the depth of the anoxic layer was evaluated. It is clear from this approach to investigating the interaction of physical and chemical aspects of sediment and water that using sediments retrieved from natural environments is much more appropriate, but also more problematic due to natural variability of a number of factors including sediment mineralogy. Relatively recent recognition of the importance of managing sediments in aquatic systems suggests that continued research on sediment-water interactions is necessary over a range of scales and in a variety of natural and controlled laboratory conditions. The following five papers reflect the type of work that should help address some current management issues.

Ellen L. Petticrew · Jennifer L. McConnachie

6.1 Identifying Variable Organic Matter Sources in Riverine Suspended Sediments

6.1.1 Introduction

The settling and storage of fine-grained sediments in the interstices of fluvial gravel beds can have significant implications on both sediment conveyance in catchments and aquatic habitat quality. Given that suspended fine-grained sediment ($<63\ \mu\text{m}$) moves not only as individual particles, but also as particle aggregates or flocs, there has been a relatively recent research emphasis on characterizing these structures and the conditions which enhance their growth and settling in freshwater aquatic environments (Kranck et al. 1993; Droppo and Ongley 1994; Petticrew 1996; Liss et al. 1996; de Boer 1997; Phillips and Walling 1999).

Flocs are comprised of both organic and inorganic material, bound together by a combination of physical, chemical, and biological forces (Droppo et al. 1997). The rate of flocculation depends on site-specific variables such as ionic and suspended sediment concentration, shear stress, pH, and organic source and supply (Droppo and Ongley 1994). This is evident in the comparison between marine and freshwater systems. Flocs are prolific in marine environments, where high concentrations have afforded them being termed “marine snow” (Alldredge and Silver 1988). Conversely, riverine flocculation is less apparent visually, and hydrologic conditions were preliminarily thought to be too energetic to facilitate floc-building. Flocculation is now a well-documented phenomenon in freshwater lotic systems (e.g., Droppo and Ongley 1994; Petticrew 1996; Phillips and Walling 1999), although the resulting particles are typically an order of magnitude smaller than their marine counterparts (e.g., 10^2 to $10^3\ \mu\text{m}$ diameter).

The main operational difference between these riverine and marine systems is ionic concentration. Flocculation in saline environments has been attributed mainly to the high electrolyte concentration (Alldredge and Silver 1988; van Leussen 1999), while freshwater systems are characterized by much lower salinity ($> 10^3\ \mu\text{S cm}^{-1}$ for marine at $25\ ^\circ\text{C}$ versus $\ll 10^3\ \mu\text{S cm}^{-1}$ for freshwater; Kalff 2002). Van Leussen (1999) states that

the role of salt flocculation is currently in question, and that organic binding agents may play an important function in the process for both environments. Droppo (2001) states that the significant biological component controlling flocculation, including both formation and destruction processes, is speculated to be organic microstructures referred to as extracellular polymeric substances (EPS). EPS appear to assist in regulating the shape and size, as well as internal complexity, of flocs by acting as bridges between inorganic particles and other components that make up floc structure. All of these morphometric characteristics inevitably influence floc density and settling velocity, which determine the nature of suspended sediment transport. EPS are typically thought of as microbial structures actively developed by microbes for several key functions. The relationship between organic matter supply and EPS is not completely understood, but the use of these structures for bacterial attachment to particles is evident (e.g., Liss et al. 1996; Droppo 2001). Dissolved and particulate organic matter must then, at the very least, have an indirect role in EPS formation as nutrients for bacterial growth and cellular activity. Both the quantity and quality of organic matter should influence the production of EPS. High quality organic matter here implies that it is readily bioavailable in that it is easily processed by microbes and metabolized efficiently. The ratio of carbon to nitrogen in organic matter has been used as means of characterizing seston quality (Bouillion et al. 2000) with lower ratios reflecting better quality, as nitrogenous products, desired by bacteria, increase. At most, organic matter could produce EPS-type molecules during decomposition that assist in particle binding in the water column. Either way, it appears that organic matter source and quality may be crucial in regulating the development of freshwater flocs. Temporal variability in floc morphology may therefore be due to changes in the sources of inorganic and organic material. Investigation of this idea requires accurate definition of organic sources and an estimate of their residence time in the aquatic system.

The use of stable isotope analysis to differentiate organic source material has increased dramatically in recent years (Griffiths 1998; Phillips and Gregg 2001). Stable isotopic tracers have been used to monitor flows of organic matter (i.e., trace trophic relations) in marine (Peterson et al. 1985; Cifuentes et al. 1988; Fry 1988; Hedges et al. 1988) and freshwater systems (Bunn et al. 1989; France 1995). Others (e.g., Kline et al. 1990; Bilby et al. 1996; Ben-David et al. 1998; McConnachie and Petticrew 2006) have utilized this technique to characterize the introduction of marine nutrients into freshwater environments. The ultimate goal of this technique is to determine the proportional contributions of multiple sources of organic matter to a mixture found in nature. Linear mixing models are used for this purpose to examine two source, single isotope, or three source, dual isotope, signatures (Phillips 2001; Phillips and Gregg 2001).

Riverine Sources of Organic Matter

Organic material introduced to river/stream ecosystems is classified as being derived from either autochthonous (generated within the stream) or allochthonous (generated from the watershed) sources. Both of these sources vary temporally and spatially. Seasonal variation of terrestrial sources is attributed to the presence of species and hydrologic regime. The composition of the riparian species changes over time, as does the proportional species contribution to streams (Johnson and Covich 1997). Stage height

and precipitation also facilitate transfer of terrestrial material to streams (Koetsier et al. 1997; Tockner et al. 1999), both laterally and longitudinally. Hydrological conditions regulate the in-stream presence and distribution of biological organisms (e.g., periphyton and invertebrates) (Allan 1995), the transport and transfer of solutes (e.g., ions and nutrients) (Webster and Ehrman 1996), and the provenance and movement of organic material (Minshall et al. 1985). Water temperature, which is intimately linked to air temperature, varies both seasonally and diurnally, as well as among locations due to regional differences in climate, elevation, extent of streamside vegetation, and relative importance of groundwater inputs (Allan 1995). In-stream production of algae and periphyton is dependent on environmental factors such as insolation and temperature (Allan 1995; Sand-Jensen 1998), as well as terrestrial nutrients.

Not only do hydrological factors affect the relative proportion of various sources of organic material, but the seasonal availability of source types does as well. As floodplains are inundated during overbank flow periods, stored organic matter may enter the stream. This occurs during episodic events such as spring melt (i.e., freshet) and rain events. Rain, and associated wind, has an added impact in that allochthonous material may get blown into the stream from riparian areas. Autochthonous sources are linked to several environmental factors, including temperature, light intensity, available nutrients, and discharge, where favorable conditions are more likely to occur during low flow periods. Allochthonous sources often follow seasonal lifecycles, where leaves and needles are shed in autumn, and new growth does not occur again until spring. A third source of organic matter exists in many watersheds that are linked to marine environments. Anadromous salmon, migrating upstream to spawn, are known to introduce important marine-derived nutrients to freshwater systems (Bilby et al. 1996). Spawning female salmon create redds, or nests for eggs, by digging up gravels, simultaneously leaving a depression for deposition of eggs and sperm. By excavating the nest they clean out fine material stored in interstitial spaces that may hinder oxygen

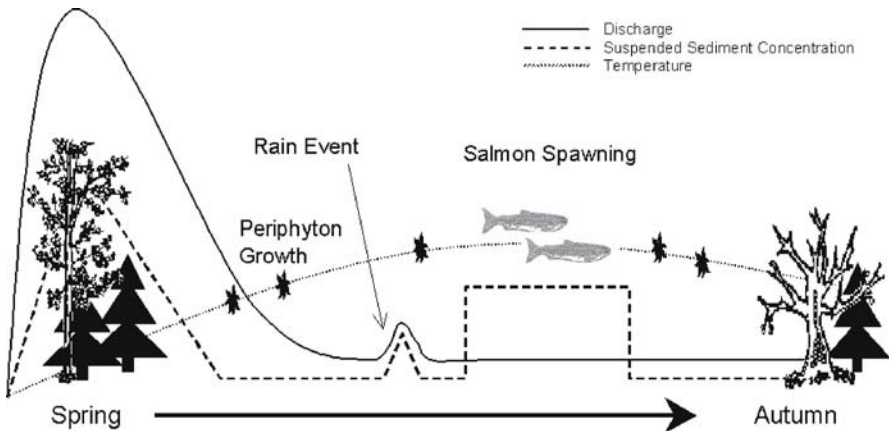


Fig. 6.1. A hypothetical depiction of seasonal patterns of suspended sediment concentration, discharge, and temperature as well as the factors which influence them in a temperate, nival dominated, fish-bearing stream. While only one rain event is shown, several typically occur during the season. Relative and absolute relationships between the variables depicted here are approximate

transfer for eggs (Soulsby et al. 2001). After spawning the female covers the eggs with excavated gravels thereby generating highly permeable sediments in the redd. Shortly thereafter (days) both the female and male die and the carcasses are left to rot in-stream providing a pulse of bioavailable, marine-derived nutrients. Figure 6.1 depicts a generalized model for these dominant sources and the timing of organic matter along with the hypothetical pattern for inorganic sediment concentrations in a typical snow-melt-dominated stream system.

Study Objective, Rationale and Approach

The objective of the work presented here was to evaluate the seasonal changes in the dominant type of organic matter incorporated in the suspended sediment of a productive fish-bearing, temperate stream system. The assumption is that in temperate forest areas such as the study region, the quality and quantity of organic material incorporated into the stream system varies over the season depending on the source types available, hydrologic regime, and conditions for biological processing. Organic matter of good quality, and/or high concentrations, may significantly increase the size of flocs, resulting in faster settling rates. This may be attributed to two factors: (1) flocculation is directly facilitated by the organic matter, or macromolecules comprising organic material; and/or (2) organic matter provides the nutrients and habitat for bacteria, which exude polymeric fibrils that bind particles together (Droppo et al. 1997).

The approach used to characterize organic matter sources was the measurement of regular carbon and nitrogen content along with stable isotopes of carbon and nitrogen in suspended sediment collected over one open-water season in a productive salmon-bearing stream. The sampling strategy was intended to capture important hydrologic and biologic events within the study system, which would influence the input and transport of various organic matter sources. Samples were collected (1) for springmelt and baseflow to allow for comparison between instances of minimum and maximum suspended material, (2) for summer rain events to incorporate resuspension of material from the bed gravels, and (3) for periods when different organic sources were evident (e.g., spawning salmon). Further work on the effect of the organic matter type of aggregate size was also undertaken but is not presented here.

6.1.2 Methods

Study Site

The study watershed of O'Ne-eil Creek (Fig. 6.2) is located in the Hagem Range of the Omenica Mountains in the Takla Lake region of northern British Columbia, Canada. As part of the most northern extent of the Fraser River watershed (55° N, 125°50' W), O'Ne-eil (also known as Kynoch) basin features a range in relief from 700–1980 m above sea level. Surficial material is comprised of glacial tills and lacustrine clays at higher elevation and fine-grained glaciolacustrine sediment in the lowland areas (Ryder 1995). Encompassed within the Engelmann Spruce Sub-alpine Fir (ESSF) biogeoclimatic zone, the basin is relatively small (~75 km²), but O'Ne-eil Creek is an

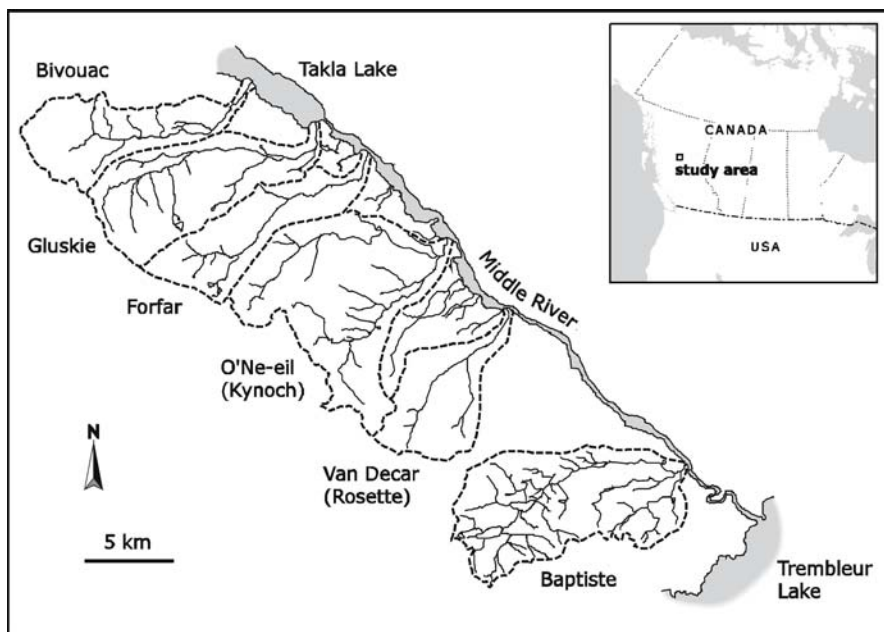


Fig. 6.2. Map of the Stuart-Takla region of northern British Columbia. Note O'Ne-eil watershed in the center

important fish-bearing stream, where annual migration of Pacific sockeye (*Oncorhynchus nerka*) salmon is well documented by Canadian Department of Fisheries and Oceans (DFO). The mainstem channel of O'Ne-eil Creek is approximately 20 km in length and 10 to 12 m wide at the mouth. The study reach exhibits favorable spawning habitat with appropriate substrate size distribution in low gradient (0.5–2%) riffles (Petticrew 1996). Little anthropogenic disturbance has occurred within this watershed specifically, however, a forest service road enables access to the lower reaches. One site in O'Ne-eil Creek, downstream of the forestry access bridge, and approximately 1 500 m upstream of the mouth, was sampled during the period of May 18 to August 21, 2001. River stage levels were monitored continuously by DFO using a pressure transducer and used in conjunction with rating curves to determine discharge. DFO also maintained precipitation gauges in the area.

Earlier quantification of organic matter inputs to the Stuart-Takla streams for 1996 by Johnston et al. (1998) indicate that riparian litter inputs for the period between July and October varied between 10 and 300 g m⁻² in dry weight, with the majority being of deciduous rather than coniferous origin. The magnitude of vegetation introduced to the streams decreased logarithmically with distance from stream banks, while the mean areal loadings decreased as channel width increased. In-stream productivity in the form of benthic algal biomass increased in late summer in response to introduction of salmon carcass derived nutrients. Johnston et al. (1998) report that the organic inputs from the in-stream rotting of salmon carcasses exceeded those of riparian leaf litter in Stuart-Takla streams.

Sample Event Selection

This study was designed to determine what type of organic matter was associated with stream suspended sediment over one open water season in O’Ne-ail Creek. In order to evaluate the seasonal changes in fine sediment composition it is necessary to collect samples over a range of watershed events which transport or deliver inorganic and organic matter. These were partitioned into five discrete event types, including: (1) springmelt during the period of rising water levels; (2) summer pre-spawn flow conditions, but isolated from rain events; (3) rain events; (4) the period during active spawning; and (5) post-spawn, where no actively spawning or live salmon were present but decay of carcasses occurred. Springmelt is a period characterized by high discharge, and this is when material stored in-channel and on the floodplain is first flushed through the system resulting in elevated suspended particulate matter levels. Less suspended load is moved during lower flow levels associated with pre-spawn flows, where the source material is predominantly in-stream. Rain events are characterized by higher than baseflow discharge, where suspended sediment concentrations are expected to increase, and potentially comprise a combination of in-stream and terrestrial inputs. Five rain events were sampled during pre-spawn, salmon spawn, and post-spawn, so they reflect the combined effects of resuspension of gravel-stored material that occurs during storms and the predominant source of organic matter for the particular sampling date. The period of active salmon spawn combines the introduction of anadromous organics and biological disturbance of gravels due to the digging of redds. Decaying salmonid organic matter is expected to be delivered to the system post-spawn, but, because live fish are no longer present, disturbance of gravels is minimal. Seasonal patterns of suspended particulate matter and suspended organic matter concentration, as well as their carbon and nitrogen signatures were identified by replicate sampling (3–5 dates) within each of the above stated event types.

Suspended Sediment Collection

A mixture of sediment and water was collected using wide-mouthed 1-l Nalgene bottles from a designated site in a well-mixed portion of the stream channel. The bottles were transported to the field laboratory where values of suspended particulate matter (SPM) and suspended organic matter (SOM) concentrations were obtained through gravimetric determination. The bottles were mixed well to obtain representative samples and then a known volume of stream water was filtered through pre-combusted and pre-weighed 47 mm diameter glass-fiber filters with a nominal pore size of 0.7 μm . Triplicate samples were filtered, dried at $\sim 60^\circ\text{C}$ and then weighed to allow the calculation of SPM concentration. The filters were then ashed in a muffle furnace at 550°C for an hour to remove the organic material and then reweighed, allowing for determination of SOM concentration.

Stable Isotopes of Carbon and Nitrogen

Stable isotope mass spectrometry (University of British Columbia, School of Oceanography Stable Isotope Laboratory) was used to characterize seasonal sources of organic

matter. The isotope ratios for both organic tissue and suspended sediment filters were measured and expressed relative to conventional standards as δ values defined as:

$$\delta X (\text{‰}) = (R_{\text{sa}}/R_{\text{std}} - 1) \times 1000 \quad (6.1)$$

where X is ^{13}C or ^{15}N , R_{sa} is the isotopic ratio of the sample (either $^{13}\text{C}/^{12}\text{C}$ or $^{15}\text{N}/^{14}\text{N}$), and R_{std} is the isotopic ratio of the standard (PeeDee Belemnite for carbon and air for nitrogen). The technique enables assessment of seasonal distribution of organic matter sources by comparing isotopic ratios from collected source material with those from suspended sediment samples. Regular carbon and nitrogen content (^{12}C and ^{14}N) was measured prior to stable isotopes in order to calculate the sample's C:N ratios. This ratio is often used to estimate sources for organic matter because autochthonous material exhibits much lower values (<15) than allochthonous material (Owen et al. 1999).

Tissue from terrestrial vegetation (e.g., spruce needles and birch, willow, and alder leaves), in-stream periphyton and algae, and salmon flesh was collected and stored in 1.2 ml centrifuge tubes and freeze-dried. Isotopes of carbon and nitrogen, as well as routine C:N ratios, were determined for each of these source materials. It should be noted that algae and periphyton are classified separately here even though the term benthic algae typically incorporates both. The algae collected for this study was free-floating and visually distinguishable from periphyton.

Duplicate samples of suspended sediment were collected, as indicated above, for isotope analysis and filtered onto pre-combusted and pre-weighed glass fiber filters, which were freeze-dried and analyzed as per the tissue samples. Seasonal trends were assessed using both carbon and nitrogen isotopes and ratios of percentage carbon and nitrogen for these filter samples.

A dual isotope (C, N), three end-member (algae, salmon, and terrestrial vegetation) mixing model based on mass balance equations (Phillips and Gregg 2001) was used to define these trends more quantitatively, and to examine relationships more conclusively. The spreadsheet used to determine source proportions, variances, standard errors, and confidence intervals can be accessed at <http://www.epa.gov/wed/pages/models.htm>.

6.1.3 Results

O'Ne-iel Creek discharge, local precipitation and the timing of sampling events are shown in Fig. 6.3a. Figure 6.3b indicates the concentrations of suspended particulate matter and suspended organic matter observed over the open water period. In 2001 the springmelt discharge began in late May. Five rising limb discharge dates were sampled which show elevated sediment concentrations. Flows attenuated in late June when five lower flow, lower sediment concentration, pre-spawn dates were sampled in June and early July. Five storm events were sampled over the summer season on July 7 and 9, and August 2, 3 and 21. These five events exhibited a range of suspended sediment response to the change in flows associated with precipitation. The estimated sockeye escapement was 13 893 with the fish arriving in the stream on July 20 and die-off beginning around early August. Five dates were sampled in active spawn and three in the post-spawn period.

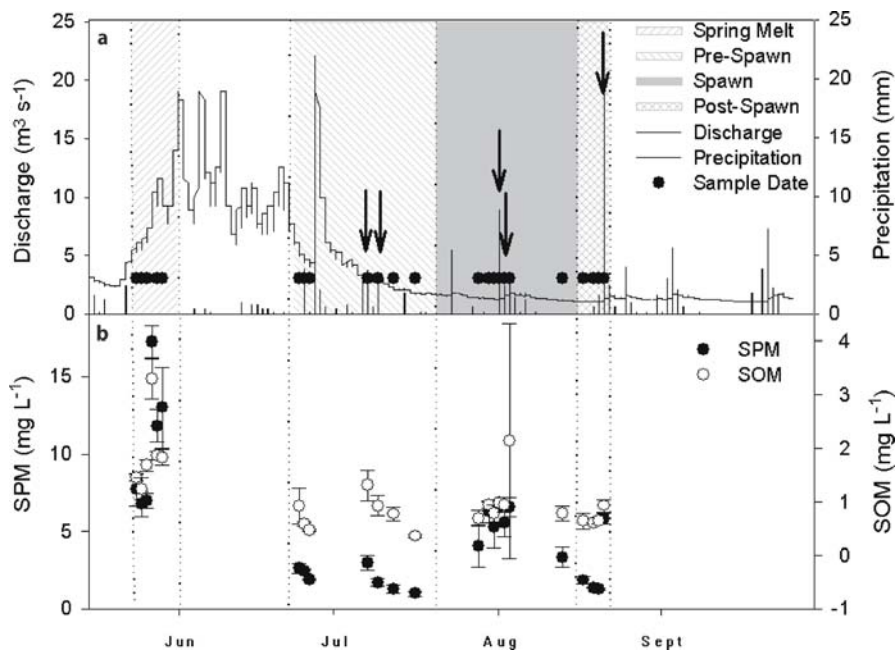


Fig. 6.3. **a** Schematic of sampling approach during the 2001 open water season. *Points* represent sampling times, *shaded areas* depict the four major event types of rising limb of springmelt, lower pre-spawn flow, and the active spawning period and post-spawn (i.e., no live/spawning salmon). *Arrows* designate sampled rain events. **b** Concentrations of SPM and SOM sampled over the open water season

Stable Isotopes of Carbon and Nitrogen

Initially, the proportion of carbon and nitrogen comprising the suspended sediment fraction was determined. Figure 6.4 shows the seasonal pattern of the ratio of carbon to nitrogen along with the discharge values. The pattern in the C:N ratio shows high values occurring during the spring period and remaining fairly constant until the salmon are introduced to the stream reach. The C:N ratio decreases while the salmon spawn and carcasses are present in-stream. The post-spawn samples are significantly different ($P < 0.05$) from both spring melt and pre-spawn samples. Figure 6.5 provides a breakdown of the C:N ratios for tissue types sampled as source material within and adjacent to O'Ne-ail Creek over the season. Mean values for tissue samples taken several times over the season of allochthonous, or terrestrially derived, vegetation exhibits C:N ratios greater than 15, ranging from $18.4 \pm 1.23\%$ for willow leaves to $41.9 \pm 7.42\%$ for spruce needles.

Autochthonous, or in-stream, organic matter is characterized here by ratios < 15 ; the lowest values being for salmon flesh with $3.4 \pm 0.07\%$, while periphyton and algae ratios are 8.3 ± 1.22 and $9.2 \pm 0.21\%$, respectively.

Stable isotope analysis of O'Ne-ail Creek source materials were undertaken on the same samples as those measured for C:N ratios that are portrayed in Figure 6.5. Statistically different carbon and nitrogen isotopic signatures were found for the three main groups of organic source material allowing for source separation techniques. Allochtho-

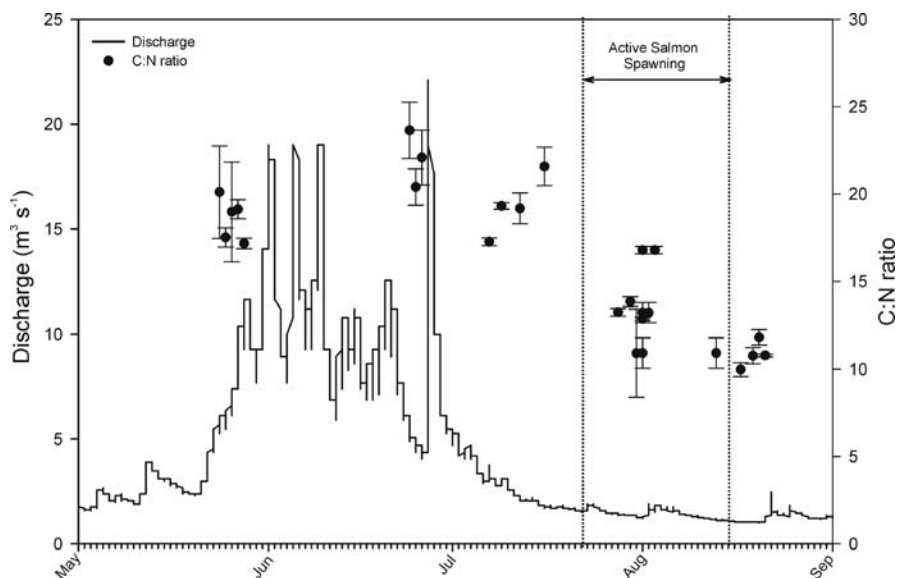
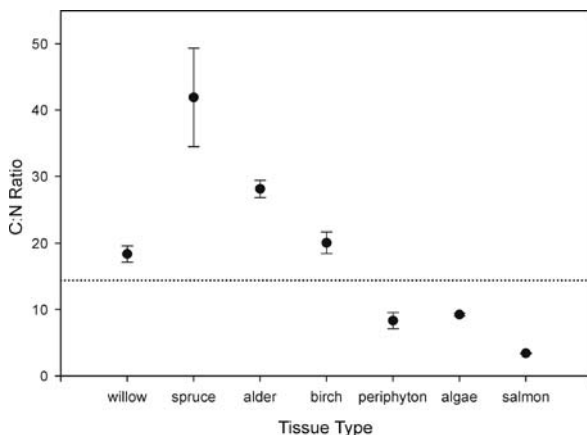


Fig. 6.4. Seasonal trend in C:N ratio of suspended sediment. *Dotted lines* indicate active spawning start (July 20) and end (August 15) dates. *Error bars* are ± 1 SE

Fig. 6.5.

Averaged C:N ratios for different types of organic source material sampled in or adjacent to O’Ne-eil Creek. *Dotted line* separates allochthonous (terrestrially derived) from autochthonous (produced in-stream) organic material



nous (terrestrial) material had a $\delta^{13}\text{C}$ value of $28.8 (\pm 0.94)$ and a $\delta^{15}\text{N}$ value of $1.1 (\pm 2.68)$. Autochthonous (algae) material had a $\delta^{13}\text{C}$ value of $21.0 (\pm 0.50)$ and a $\delta^{15}\text{N}$ value of $10.8 (\pm 0.09)$. The salmonid samples had a $\delta^{13}\text{C}$ value of $35.3 (\pm 0.76)$ and a $\delta^{15}\text{N}$ value of $0.5 (\pm 0.25)$ (Table 6.1). Seasonal analysis of the mixture of organic material in the suspended sediment reveals a trend of enrichment of the stable (heavier) isotope over the season for both carbon and nitrogen, although the latter is much more pronounced (Fig. 6.6). A slight increase in carbon isotope ratio is seen from springmelt to low flow with $\delta^{13}\text{C}$ values of -26.8 ± 0.09 and $-26.6 \pm 0.10\%$, respectively. Once salmon enter the reach, the isotopic signal increases to $-26.1 \pm 0.18\%$. The

Table 6.1. Partitioning of organic matter source contributions to suspended sediment load in O’Ne-eil Creek as modeled for the five event types of springmelt, pre-spawn flow, rain events, spawn, and post-spawn using dual isotopic signatures ($\delta^{13}\text{C}$ and $\delta^{15}\text{N}$). Note that the model used here limits the total percentage of the three sources types to be 100. This explains the presence of negative values to balance those that are >100%

	Mixture (Sediment)	Terrestrial vegetation	Salmon flesh	Algae
Springmelt				
$\delta^{13}\text{C}$ (‰) (SE)	-26.8 (0.06)	-28.8 (0.94)	-21.0 (0.50)	-35.3 (0.76)
$\delta^{15}\text{N}$ (‰) (SE)	2.0 (0.11)	1.1 (2.68)	10.8 (0.09)	0.5 (0.25)
Sample size	10	14	4	3
Source proportions (%) (SE) – calculated		110.9 (20.0)	8.7 (8.8)	-19.7 (11.6)
95% confidence limits (%)		68.4–100	0–27.8	0–4.5
Pre-spawn flow				
$\delta^{13}\text{C}$ (‰) (SE)	-26.6 (0.07)	-28.8 (0.94)	-21.0 (0.50)	-35.3 (0.76)
$\delta^{15}\text{N}$ (‰) (SE)	2.4 (0.09)	1.1 (2.68)	10.8 (0.09)	0.5 (0.25)
Sample size	10	14	4	3
Source proportions (%) (SE) – calculated		105.8 (19.0)	12.9 (8.4)	-18.6 (11.0)
95% Confidence limits (%)		65.3–100	0–31.0	0–4.4
Rain events				
$\delta^{13}\text{C}$ (‰) (SE)	-26.2 (0.11)	-28.8 (0.94)	-21.0 (0.50)	-35.3 (0.76)
$\delta^{15}\text{N}$ (‰) (SE)	3.8 (0.31)	1.1 (2.68)	10.8 (0.09)	0.5 (0.25)
Sample size	10	14	4	3
Source proportions (%) (SE) – calculated		80.8 (16.5)	27.1 (7.3)	-7.9 (9.5)
95% confidence limits (%)		46.6–100	11.8–42.4	0–11.6
Spawn				
$\delta^{13}\text{C}$ (‰) (SE)	-26.2 (0.11)	-28.8 (0.94)	-21.0 (0.50)	-35.3 (0.76)
$\delta^{15}\text{N}$ (‰) (SE)	4.3 (0.38)	1.1 (2.68)	10.8 (0.09)	0.5 (0.25)
Sample size	10	14	4	3
Source proportions (%) (SE) – calculated		68.6 (15.7)	32.8 (7.0)	-1.4 (9.0)
95% confidence limits (%)		36.2–100	18.3–47.2	0–17.1
Post-spawn				
$\delta^{13}\text{C}$ (‰) (SE)	-25.6 (0.07)	-28.8 (0.94)	-21.0 (0.50)	-35.3 (0.76)
$\delta^{15}\text{N}$ (‰) (SE)	5.6 (0.18)	1.1 (2.68)	10.8 (0.09)	0.5 (0.25)
Sample size	6	14	4	3
Source proportions (%) (SE) – calculated		46.0 (9.5)	46.8 (4.1)	7.2 (5.7)
95% confidence limits (%)		26.2–65.8	38.1–55.5	0–18.9

peak of enrichment occurs just prior to the post-spawn period, where some salmon are still alive, but earlier returns have already begun to rot in situ. After this, the isotopic ratio decreases towards a signal more similar to the period prior to salmon presence;

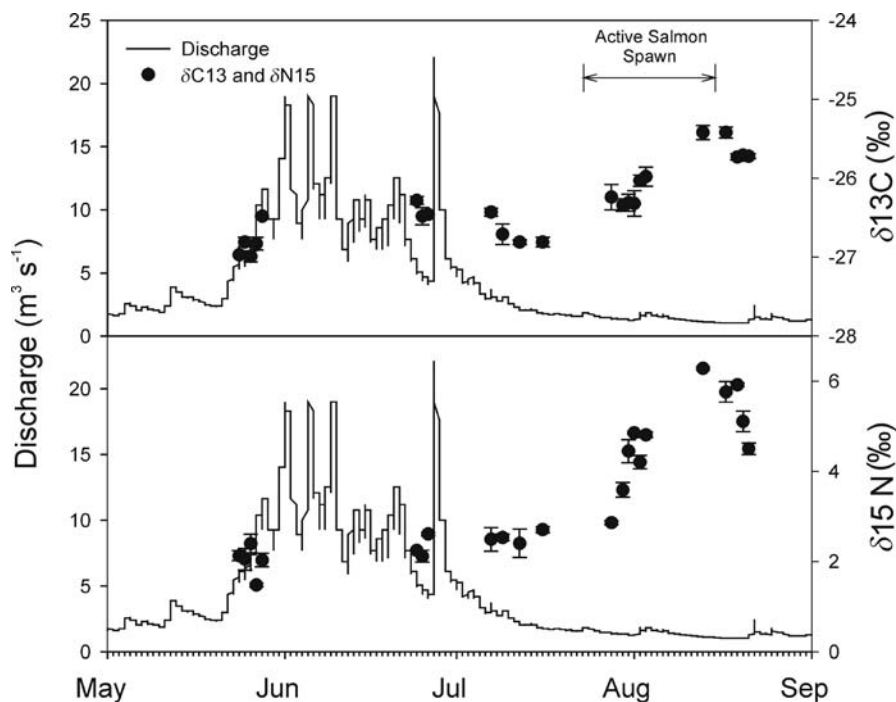


Fig. 6.6. Seasonal trends for stable isotopes of carbon and nitrogen from suspended sediment. The salmon spawning period is designated. Error bars are ± 1 SE

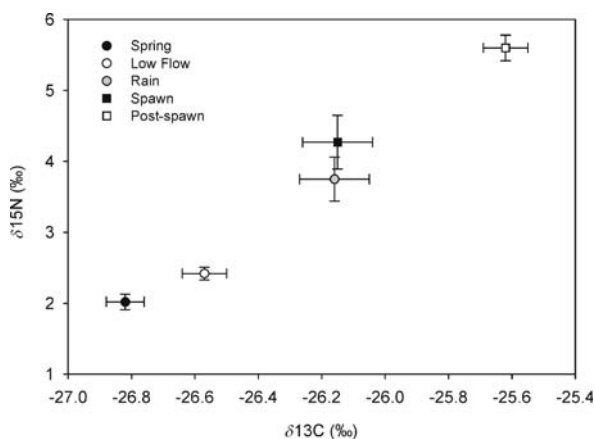
however, the measured trend ends before the decline is complete, so the grouped average for the post-spawn event shows the highest enrichment as compared to all other event types ($-25.6 \pm 0.07\text{‰}$). The nitrogen isotope exhibits a similar pattern with enrichment of $\delta^{15}\text{N}$ from springmelt to pre-spawn flow of 2.02 ± 0.11 to $2.42 \pm 0.09\text{‰}$, a steep increase over the active salmon spawning period with an average of $4.27 \pm 0.38\text{‰}$, and further enrichment after salmon die-off is complete ($5.60 \pm 0.18\text{‰}$).

The combined results of the two isotopic elements are typically shown as in Fig. 6.7, and there is clearly an increasing trend, where springmelt < low flow < rain \approx spawn < post-spawn. Rain events were sampled over three different event types (pre-spawn flow, spawn, and post-spawn), and the average is approximately equal to that of the salmon period due to the linearity of the relationship observed in these event types (Figure 6.7). In fact, linear regression was applied to the semi-logged ungrouped data, and the relationship is significant with $r^2 = 0.663$ for $N = 46$ and $\alpha = 0.05$.

For modeling purposes, the data derived from the suspended sediment filters were compared to the tissue samples, using the dual isotope, three end-member format developed by Phillips and Gregg (2001). The results indicate that the predominant source of organic matter to the suspended sediment load changed over the season, although the 95% error bars are very large (Table 6.1). For the springmelt period, the model suggests that all organic material is derived from terrestrial vegetation, while the salmon and algal sources are contributing minimal amounts to the suspended sediment sup-

Fig. 6.7.

Stable isotopes for suspended sediment filters as grouped by event type. Bi-directional error bars are ± 1 SE for both variables



ply. Similarly, terrestrial vegetation dominates as the organic source for the pre-spawn suspended sediments. A shift begins toward a positive salmon contribution for the rain events category, with between 66 and 95% of the proportion remaining terrestrially derived, and 21 to 34% being of salmon origin. The divergence continues for the active salmon spawn, where the suspended sediment samples were composed of anywhere from 56 to 81% of vegetative tissue, 27 to 38% of salmon flesh, and 0 to 6.1% of algae. The post-spawn period was characterized by an overlap of terrestrial and salmon inputs, $46.0\% \pm 8.6$ and $46.8 \pm 3.7\%$, respectively, and minimal algal inputs ($7.2 \pm 5.2\%$). Periphyton was excluded from the model because it utilizes nutrients from the water column (Johnston et al. 1998), which complicates modeling because the periphyton isotopic signature is then a mixture of the end-members. Phillips and Gregg (2001) suggest that samples from the three source populations should be independent.

6.1.4 Discussion and Conclusion

Both the carbon to nitrogen ratios and the stable isotope analysis of suspended sediment reflect differences in organic matter composition seasonally. The changing signal of C:N from suspended sediment filters indicates the sediment load response to the seasonal change in organic matter type. Figure 6.4 displays the transitional decrease in C:N ratio caused by salmon presence within the study reach from a ratio greater than 15 to a ratio less than 15. This dilution of C:N ratios through the addition of autochthonous (i.e., in-stream) matter results in much lower values than those of allochthonous (i.e., terrestrially derived) materials that dominate earlier in the season. Figure 6.5, showing the C:N ratios for terrestrial- versus aquatic-derived organic source material for O'Ne-eil Creek, confirms this, as terrestrial sources are characterized by ratios greater than 15, whereas the in-stream supply falls below 15 as suggested by Owen et al. (1999). Thus, it appears that the suspended sediment load adopts an elemental signal related to changing type of source material. Although the ratio does not decrease as far as to match the measured ratio for salmon flesh, the presence of salmon detritus is detectable in the suspended sediment load when stable isotopes are used.

It is clear that stable isotopes provide more specific information for characterizing organic matter sources and differentiating the timing of their contribution to the stream system. Different types of organic tissue exhibit distinctly different isotopic signals, which enables differentiation between samples and even the tracing of trophic pathways through systems (Fry 1988). The data presented in Fig. 6.6 indicates little temporal variation in $\delta^{13}\text{C}$ (-27 to -26‰) and $\delta^{15}\text{N}$ (2 to 3‰) until the salmon enter the reach. At this point, a steep increase in the heavier isotopes of each element occurs; steeper for nitrogen than carbon. Then, when live salmon are no longer present in the stream, both carbon and nitrogen isotopes fall off; probably as salmon-introduced nutrients from decay processes are utilized or flushed downstream. This trend is supported by Ben-David et al. (1998), who reported that spawning Pacific salmon exhibit higher proportions of heavier carbon and nitrogen isotopes ($\delta^{13}\text{C} = -18.65 \pm 0.18\text{‰}$ and $\delta^{15}\text{N} = 13.01 \pm 0.13\text{‰}$) than terrestrial plants (means of $\delta^{13}\text{C} \approx -27\text{‰}$ and $\delta^{15}\text{N} \approx 0\text{‰}$; France 1997). Isotopic content of the event groups is clearly differentiated in Fig. 6.7 indicating the usefulness of this method in distinguishing suspended sediment organic matter types. The role of decaying salmon in introducing marine derived nutrients to the stream is supported in this data set by the elevated values during post-spawn.

Dual isotope, three end-member modeling corroborates the visual stable isotope pattern (Fig. 6.7), although a significant amount of variation in proportion of contributors exists (Table 6.1). Phillips and Gregg (2001) performed sensitivity analysis of this linear mass balance model. They found that large differences in isotopic signal between sources reduced the error (i.e., doubling the difference reduced the uncertainty by half). Further, sample size is important when dealing with source samples exhibiting similar isotopic signatures. Thus, increasing the number of samples collected, especially for terrestrial vegetation, which varies significantly in terms of species and season (France 1995), should improve the resolution of this model. As well, collecting tissue samples in a more continuous manner over the season, rather than the episodic approach presented here, and applying the model to sources collected at the same time as the mixture, may also assist investigation of natural patterns.

The stable isotope analysis substantiates earlier indications that organic source type is of significant importance for flocculation in O'Ne-eil Creek (McConnachie and Petticrew 2006). The observed contributions of organic matter to the suspended sediment follows the general pattern of terrestrial and in-stream contribution as depicted in the schematic of Fig. 6.1. Other reported results from this study area indicate larger aggregate particles were found during salmon spawn and decay (Petticrew 1996; McConnachie 2003; Petticrew and Arocena 2003; McConnachie and Petticrew 2004), a time when the dominant organic source type changes from terrestrial material to higher quality, marine-derived organic matter introduced to the freshwater system by the salmon vector. Both carbon and nitrogen signals changed considerably in terms of the heavier isotopes for the spawn compared to the pre-spawn flow period; however, samples taken up to mid-July were equal to or less than the springmelt concentrations, indicating a predominance of the terrestrial organic matter over that period.

The relationship between organic content and particle morphology, when sampled in a natural environment, is confounded by the range of variables (e.g., shear velocity, temperature) influencing aggregate size and stability, which make it difficult to isolate the influence of organic matter source material. However, laboratory evaluations indi-

cate that the quality of the organic matter, as it relates to a suitable bacterial substrate, influences the floc development due to bacterial EPS. Therefore, characterizing the temporal and spatial changes of organic contributions is an important factor in assessing riverine sediment storage and transfers.

Acknowledgments

The opportunity to attend the Sedymo Conference in Harburg, Germany and to participate in this book was made possible by Ulrich Förstner. An initial review of the paper by Philip Owens is much appreciated. The field assistance of Antje Ullrich and Beka McConnachie is acknowledged as are sample analysis and laboratory assistance provided by Leslie Chamberlist and Tauqeer Waqar. This work was undertaken as part of the larger Stuart-Takla Fisheries-Forestry Interaction Project. Hydrologic data and field facilities were donated by the Canadian Department of Fisheries and Oceans, and Canadian Forest Products. Funding for this work was provided by Natural Science and Engineering Research Council to both authors and the Northern Land Use Institute and Fisheries Renewal British Columbia grants to ELP.

References

- Allan JD (1995) Stream ecology: structure and function of running waters. Chapman and Hall, London
- Allredge AL, Silver MW (1988) Characteristics, dynamics and significance of marine snow. *Progress in Oceanography* 20:41–82
- Ben-David M, Hanley TA, Schell DM (1998) Fertilization of terrestrial vegetation by spawning Pacific salmon: the role of flooding and predator activity. *Oikos* 83:47–55
- Bilby RE, Franssen BR, Bisson PA (1996) Incorporation of nitrogen and carbon from spawning coho salmon into the trophic system of small streams: evidence from stable isotopes. *Canadian Journal of Fisheries and Aquatic Sciences* 53:164–173
- Bouillon S, Mohan PC, Sreenivas N, Dehairs F (2000) Sources of suspended organic matter and selective feeding by zooplankton in an estuarine mangrove ecosystem as traced by stable isotopes. *Marine Ecology Progress Series* 208:79–92
- Bunn SE, Barton DR, Hynes HBN, Power G, Pope MA (1989) Stable isotope analysis of carbon flow in a tundra river system. *Canadian Journal of Fisheries and Aquatic Sciences* 46:1769–1775
- Cifuentes LA, Sharp JH, Fogel ML (1988) Stable carbon and nitrogen isotope biogeochemistry in the Delaware Estuary. *Limnology and Oceanography* 33:1102–1115
- de Boer DH (1997) An evaluation of fractal dimensions to quantify changes in the morphology of fluvial suspended sediment particles during baseflow conditions. *Hydrological Processes* 11:415–426
- Droppo IG (2001) Rethinking what constitutes suspended sediment. *Hydrological Processes* 15:1551–1564
- Droppo IG, Ongley ED (1994) Flocculation of suspended sediment in rivers of southeastern Canada. *Water Research* 28:1799–1809
- Droppo IG, Leppard GG, Flannigan DT, Liss SN (1997) The freshwater floc: a functional relationship of water and organic and inorganic floc constituents affecting suspended sediment properties. *Water, Air and Soil Pollution* 99:43–45
- France RL (1995) Critical examination of stable isotope analysis as a means for tracing carbon pathways in stream ecosystems. *Canadian Journal of Fisheries and Aquatic Sciences* 52:651–656
- France RL (1997) Stable carbon and nitrogen isotopic evidence for ecotonal coupling between boreal forests and fishes. *Ecology of Freshwater Fish* 6:78–83
- Fry B (1988) Food web structure on Georges Bank from stable C, N, and S isotopic compositions. *Limnology and Oceanography* 33:1182–1190

- Griffiths H (1998) Stable isotopes, integrations of biological, ecological and geochemical processes (Environmental Plant Biology Series). Bios, Oxford
- Hedges JJ, Clark WA, Cowie GL (1988) Organic matter sources to the water column and surficial sediments of a marine bay. *Limnology and Oceanography* 33:1116–1136
- Johnson SL, Covich AP (1997) Scales of observation of riparian forests and distributions of suspended detritus in a prairie river. *Freshwater Biology* 37:163–175
- Johnston NT, Fuchs S, Mathias KL (1998) Organic matter sources in undisturbed forested streams in the north-central interior of BC. Riparian Ecosystems Research Program Newsletter. Forest Renewal BC, Canada
- Kalff J (2002) *Limnology: inland water ecosystems*. Prentice Hall, New Jersey
- Kline TC, Goering JJ, Mathisen OA, Poe PH, Parker PL (1990) Recycling of elements transported upstream by runs of Pacific salmon: I. $\delta^{15}\text{N}$ and $\delta^{13}\text{C}$ evidence in Sashin Creek, southeastern Alaska. *Canadian Journal of Fisheries and Aquatic Sciences* 47:136–144
- Koetsier P, McArthur JV, Leff LG (1997) Spatial and temporal response of stream bacteria to sources of dissolved organic carbon in a blackwater stream system. *Freshwater Biology* 37:79–89
- Kranck K, Petticrew EL, Milligan TG, Droppo IG (1993) In situ particle size distributions resulting from flocculation of suspended sediment. *Coastal and Estuarine Study Series* 42:60–74
- Liss SN, Droppo IG, Flannigan D, Leppard GG (1996) Floc architecture in wastewater and natural riverine systems. *Environmental Science and Technology* 30:680–686
- McConnachie JL (2003) Seasonal variability of fine-grained sediment morphology in a salmon-bearing stream. M.S. Thesis, University of Northern British Columbia, Prince George
- McConnachie JL, Petticrew EL (2004) Hydrological and biological event based variability in the fine-grained sediment structure of a small undisturbed catchment. In: Golosov V, Belyaev V, Walling DE (eds) *Sediment transfer through the fluvial system*. IAHS Pub 288. IAHS Press, Wallingford, pp 459–465
- McConnachie JL, Petticrew EL (2006) Tracing organic matter sources in riverine suspended sediment: Implications for fine sediment transfers. *Geomorphology* 79:13–26
- Minshall GW, Petersen RC, Cummins KW, Bott TL, Sedell JR, Cushing CE, Vannote RL (1985) Interbiome comparison of stream ecosystem dynamics. *Ecological Monographs* 53:1–25
- Owen JS, Mitchell MJ, Michener RH (1999) Stable nitrogen and carbon isotopic composition of seston and sediment in two Adirondack Lakes. *Canadian Journal of Fisheries and Aquatic Sciences* 56:2186–2192
- Peterson BJ, Howarth RW, Garritt RH (1985) Multiple stable isotopes used to trace the flow of organic matter in estuarine food webs. *Science* 227:1361–1363
- Petticrew EL (1996) Sediment aggregation and transport in northern interior British Columbia streams. In: Walling DE, Webb BW (eds) *Erosion and sediment yield: global and regional perspectives*. IAHS Pub 236. IAHS Press, Wallingford, pp 313–319
- Petticrew EL, Arocena JM (2003) Organic matter composition of gravel-stored sediments from salmon bearing streams. *Hydrobiologia* 494:17–24
- Phillips DL (2001) Mixing models in analyses of diet using multiple stable isotopes: a critique. *Oecologia* 127:166–170
- Phillips DL, Gregg JW (2001) Uncertainty in source partitioning using stable isotopes. *Oecologia* 127:166–170
- Phillips JM, Walling DE (1999) The particle size characteristics of fine-grained channel deposits in the River Exe Basin, Devon, UK. *Hydrological Processes* 13:1–19
- Ryder JM (1995) Stuart-Takla watersheds: terrain and sediment sources. Work Paper 03/1995. BC Ministry of Forests, Victoria
- Sand-Jensen K (1998) Influence of submerged macrophytes on sediment composition and near-bed flow in lowland streams. *Freshwater Biology* 39:663–679
- Soulsby C, Youngson AF, Moir HJ, Malcolm IA (2001) Fine sediment influence on salmonid spawning habitat in a lowland agricultural stream: a preliminary assessment. *Science of the Total Environment* 265:295–307
- Tockner K, Pennetzdorfer D, Reiner N, Schiemer F, Ward JV (1999) Hydrological connectivity, and the exchange of organic matter and nutrients in a dynamic river-floodplain system (Danube, Austria). *Freshwater Biology* 41:521–535
- van Leussen W (1999) The variability of settling velocities of suspended fine-grained sediment in the Ems Estuary. *Journal of Sea Research* 41:109–118
- Webster JR, Ehrman TP (1996) Solute dynamics. In: Hauer FR, Lamberti GA (eds) *Methods in stream ecology*. Academic Press Inc., San Diego, 145–160

*Fritz Hartmann Frimmel · Gudrun Abbt-Braun · George Metreveli
Markus Delay · Christian Heise*

6.2 Aggregation and Sorption Behavior of Fine River Sediments

6.2.1 Introduction

The suspension and deposition behavior of fine particles in rivers is of high environmental relevance and depends on numerous physical-chemical factors (Lick 1982). Flow turbulence, particle size distribution, particle surface charge, ionic strength, and the concentration of organic matter (OM) are key parameters associated with these processes (Amos et al. 1992; Buffle and Leppard 1995a,b). Fine particles can interact with organic and inorganic pollutants (Grolimund et al. 1996; Roy and Dzombak 1997; Kretzschmar et al. 1999) and facilitate their transport in river systems, but they also may contribute to the immobilization of pollutants due to particle sedimentation.

In this contribution, the role of different physical-chemical parameters on the aggregation behavior of fine river sediments from the river Elbe and a model solid phase (kaolin) was investigated as well as the interaction of these solid phases with inorganic pollutants (copper, lead, zinc). Focus was put on the role of organic matter, particle surface charge, and ionic strength on the aggregation and sorption behavior of the river sediment and kaolin. The aim of the work was to assess the potential impact of particle mediated transport of contaminants on river systems.

6.2.2 Materials and Methods

Sample preparation in all experiments was carried out by using demineralized water (Milli-Q Plus, Millipore). For pH adjustment and for sediment washing HCl (suprapur, Merck) and NaOH (Merck) were used.

Solid Phases

Sediment sampling and properties. Channel bed sediment samples were collected from the river Elbe at Bühnenfeld (stream km 607.5, depth: 2 m). After sample collection, pore water was separated from the sediment. To do this, sediment samples were centrifuged at 4000 rpm ($2\,150 \times g$) for 60 min (ROTANTA 460 RS, Andreas Hettich GmbH & Co KG). After centrifugation, the supernatant was filtered with $0.45\ \mu\text{m}$ membranes and analyzed for concentration of dissolved organic carbon (DOC) (Sievers 820, Portable Total Organic Carbon Analyser, Sievers Instruments Inc., USA). The centrifuged sediment was freeze-dried (1.030 mbar, $-20\ ^\circ\text{C}$; Christ, Alpha 2-4; Sed₀). A portion of the freeze-dried material was analyzed for mineral content using X-ray diffractometer (Siemens Diffrac 11). The results of X-ray diffractometry measurements are shown in Table 6.2.

To remove organic or inorganic (metal species) constituents, the freeze-dried sediment Sed₀ was washed with the following solutions and in the following order: solution of NaOH ($0.1\ \text{mol l}^{-1}$), demineralized water, solution of HNO₃ ($0.1\ \text{mol l}^{-1}$) and

Table 6.2.
Mineral content of original
(freeze-dried) sediment

Minerals	Content in % (mass/mass)
Quartz	23
Feldspar	2
Mica	32
Kaolinite	37
Swelling minerals	3
Dolomite	1
Calcite	2

demineralized water. Each washing step was carried out three times and for 24 h. Finally the washed sediment was freeze-dried (Sed_w).

Kaolin. Kaolin H 3 GF (Dorfner, $d_{50} = 3 \mu\text{m}$) was used as reference material for a mineral solid phase.

Aggregation Behavior of the Sediment

For the stability characterization of fine sediments samples of Sed_o and Sed_w were prepared with demineralized water and pore water ($n = 3$). The concentration of sediment was set to 2 g l^{-1} . In the supernatant, collected following sedimentation of the larger particles ($>1 \mu\text{m}$), pH value, electrical conductivity, particle size and zeta potential were determined. Particle size and zeta potential were measured using Zetasizer Nano ZS (Malvern Instruments, laser: 4 mW He-Ne, $\lambda = 633 \text{ nm}$). For the particle size measurements dynamic light scattering technique was used (scattering angle: 173°). The electrophoretic mobility was detected by means of the laser doppler electrophoreses. The zeta potential was calculated from electrophoretic mobility using the Smoluchowski equation (Müller 1996).

Titration experiments. For a detailed characterization of the aggregation behavior of sediment particles, titration experiments were carried out by means of a Zetasizer and an Autotitrator (MPT-2, Malvern Instruments). The titration was done in a plastic beaker, which was connected through a capillary system and a peristaltic pump with a folded capillary zeta potential cell (DTS 1060, Malvern Instruments). The sediment samples (Sed_o , Sed_w , $\rho = 2 \text{ g l}^{-1}$ each) were prepared with demineralized water. A volume of 10 ml of the supernatant, obtained after sedimentation of the larger particles ($>1 \mu\text{m}$), was titrated with solutions of MgSO_4 (0.01 ; 0.1 and 0.5 mol l^{-1}) in the concentration range from 0 mmol l^{-1} to 50 mmol l^{-1} to study the influence of the ionic strength on the aggregation of the particles. The pH value remained constant at 7 during the titration. Furthermore, the same samples were titrated from a pH value of 7 to pH 2 with HCl (0.1 mol l^{-1} and 1 mol l^{-1}) and from a pH value of 7 to 12 with NaOH (1 mol l^{-1}). After each adjustment of pH value and MgSO_4 concentration, the particle size and electrophoretic mobility was measured three times. Between the measurements and during the adjustments of pH value and MgSO_4 concentration, the sample was circulated and stirred. The titration experiments were controlled automatically by software.

Stirring tank experiments. In cooperation with the Institute for Hydromechanics, Universität Karlsruhe (TH) (Prof. G. H. Jirka, Dipl.-Ing. G. Kühn), experiments in a stirring tank were performed in order to investigate the influence of ionic strength on the aggregation behavior of fine particles. The stirring tank had a volume of 1.2 l (inner diameter: 100 mm, height: 150 mm). A MgSO_4 solution (2 mol l^{-1}) was added stepwise (20 steps of 5 ml, each) to a suspension of freeze-dried river Elbe sediment (Sed_0 ; $\rho = 250 \text{ mg l}^{-1}$). The suspension was stirred continuously (150 rpm) to prevent settling of particles.

For particle detection, an optical measurement technique based on an In-Line Microscope (Aello 7000) with a CCD camera system was used. With the instrumental set-up, particles between 4 and 500 μm could be detected.

Column Leaching Experiment and Size Exclusion Chromatography

Column leaching experiment. To examine the release of organic compounds from the river Elbe sediment, column leaching experiments were performed. A column (Alltech Grom, ECO GR-G4550Z, $450 \times 50 \text{ mm}$) filled with 600 g of the freeze-dried sediment was sequentially leached with 950 ml of the following eluents: demineralized water, solutions of MgSO_4 (0.05 and 0.01 mol l^{-1}), and a solution of NaOH (0.1 mol l^{-1}).

A HPLC unit (Amersham Pharmacia, ÄKTA Explorer 100) with pump and UV detector ($\lambda = 254 \text{ nm}$) was used at a flow rate of 1 ml min^{-1} . In the column outlet, UV absorption, pH value and electrical conductivity were detected online.

Size exclusion chromatography (SEC). For characterization of the organic matter in the eluates, the analytical SEC system LC-OCD with a TSK HW 50 S column and a phosphate buffer (0.028 mol l^{-1}) was used. The system was described in detail by Huber and Frimmel (1992). The system was also used to determine the DOC concentrations of the eluates. The DOC concentrations were calculated from bypass DOC peak areas by an external calibration of the DOC detector with potassium hydrogen phthalate as standard. Samples with a DOC above 10 mg l^{-1} were diluted with buffer prior to measurement.

Sorption of Heavy Metals

Sorption kinetics of heavy metals (Cu, Pb and Zn) on Sed_w and kaolin particles in the presence and in the absence of dissolved organic matter (DOM) were investigated in batch experiments. The metal stock solutions for the sorption experiments were prepared by using: $\text{CuCl}_2 \cdot 2\text{H}_2\text{O}$ (Merck), PbCl_2 (Merck), and ZnCl_2 (Merck). These salts were dissolved in a solution of HCl (10 mmol l^{-1}). The concentration of metals was set to 10 mmol l^{-1} . Freeze-dried sediment was dispersed and extracted with NaOH solution (0.1 mol l^{-1}) (solid to liquid ratio: $50 \text{ g}/0.5 \text{ l}$) and shaken by a vertically spinning mixer. The extract was used as solution to study the influence of dissolved organic matter (DOM) in the batch experiments. The concentration of the solid phases (sediment and kaolin) was set to 5 g l^{-1} . The heavy metal concentration ($50 \mu\text{mol l}^{-1}$) and DOM concentration (40 mg l^{-1}) were adjusted by using metal stock solutions and sediment extract respectively. 40 ml samples were shaken in plastic beakers (Greiner Bio-one) using a vertically spinning mixer (REAX 20, Heidolph).

The sorption experiments were carried out at pH values of 5 and 7. After mixing of the components three aliquot samples (3.5 ml each) were sub sampled between 1 and 500 min, transferred to the centrifuge tubes and centrifuged in an ultracentrifuge (Optima TLX, Beckman Coulter) at 100 000 rpm ($417\,000 \times g$) for 20 min. After centrifugation, 1.5 ml of supernatant from each tube was obtained. The supernatants were collected in one tube (4.5 ml), stabilized with 1% HNO_3 (suprapur, Merck) and analyzed for metal concentration with inductively coupled plasma optical emission spectrometer (ICP-OES, Vista-Pro CCD Simultaneous, Varian).

6.2.3 Results and Discussion

Aggregation Behavior of the Sediment

Both original and washed river sediment (Sed_o and Sed_w) particles dispersed in demineralized water showed a negative zeta potential between -19 mV and -21 mV (see Fig. 6.8). Due to the high ionic strength, the original and washed sediment dispersed in pore water showed a slight decrease of the negative zeta potential (-16 mV). This trend is associated with a significant increase of the particle size from 500 nm to 1 500 nm. This is due to the compression of the electrical double layer by the adsorption of cations from the pore water onto the particle surface. As a consequence of the decreasing repulsive electrostatic forces, the particles aggregate rapidly. The pH value remained constant between 7 and 8. It is interesting to note that washing of sediment particles showed no significant influence on their aggregation behavior.

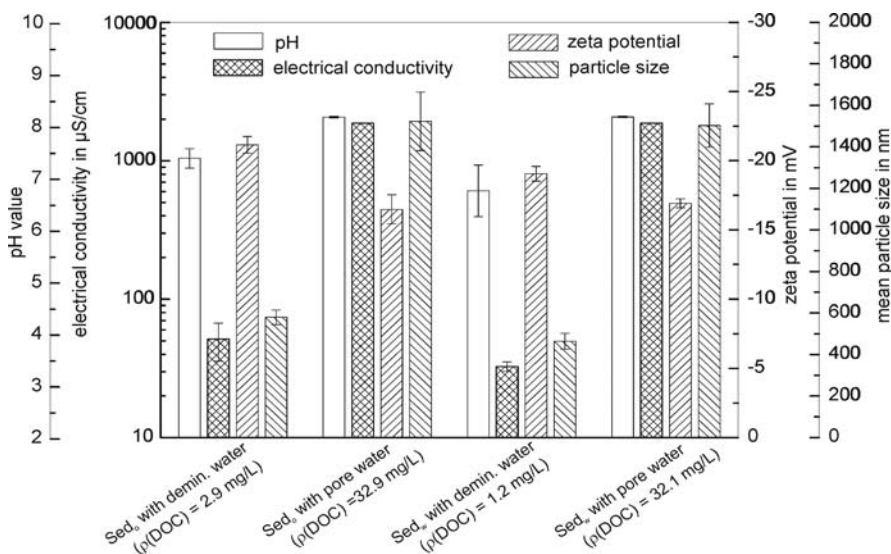


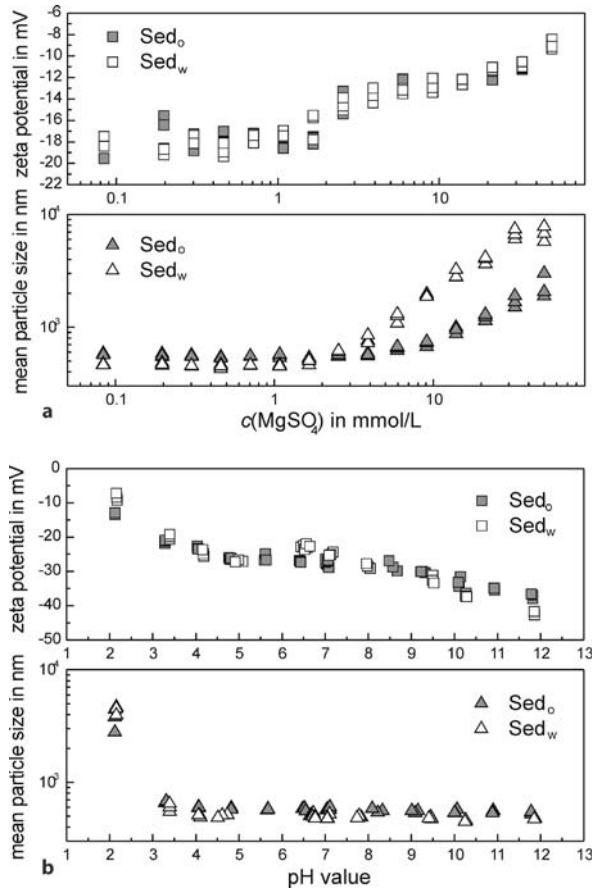
Fig. 6.8. pH value, electrical conductivity, particle size and zeta potential of original and washed river sediment (Sed_o and Sed_w) dispersed in demineralized water and pore water (DOC concentration in pore water: 31.9 mg l^{-1})

Titration experiments. The stability and aggregation behavior of fine sediment particles was investigated in titration experiments. Figure 6.9a shows the zeta potential and particle size of original and washed sediment as a function of the MgSO_4 concentration. Titration with MgSO_4 solution caused a decrease of the negative zeta potential with increasing salt concentration from -20 mV to -8 mV. The particles remain stable in the concentration range of 0 to 3 mmol l^{-1} . The increase of MgSO_4 concentration leads to aggregation of sediment particles. The aggregation for washed sediment particles was stronger than for original sediment particles. During sediment washing with the NaOH solution, a significant part of organic compounds was desorbed from the particle surface. Therefore, it is assumed that the presence of organic compounds on the surface of original sediment particles can cause their stabilization (Kretzschmar et al. 1995; Kretzschmar and Sticher 1997) such that the aggregates are smaller than for the washed sediment.

The influence of the pH value on the stability of original and washed sediment particles was also investigated in the titration experiments (Fig. 6.9b). The zeta potential remained negative (from -42 mV to -7 mV) at the pH range investigated (pH 2 to

Fig. 6.9.

Influence of MgSO_4 concentration (a) and pH value (b) on the zeta potential and mean particle size of original (Sed_o) and washed sediment (Sed_w)



pH 12) and as expected, it became less negative with decreasing pH value due to the increasing protonation of the particle surface.

The average particle size of the sediment remained stable (about 500 nm) in the pH range of 4 to 12. At lower pH values (pH 4 to pH 2), the particle size increased rapidly and sediment particles agglomerated. At pH 2, agglomerates with an average particle size of about 3 μm to 4 μm were detected. Washing showed no significant influence on the aggregation behavior of the sediment particles.

Stirring tank experiments. Additionally, stirring tank experiments were performed for the characterization of the aggregation behavior of sediment particles. Figure 6.10 shows the median particle size (d_{50}) as a function of the MgSO_4 concentration. In the stirring tank experiments, an aggregation of the sediment particles was observed. Increasing MgSO_4 concentration led to an increase of the median particle size. At high salt concentrations (100 mmol l^{-1} to 160 mmol l^{-1}), a maximal value of aggregate size was reached (about 40 μm).

Column Leaching Experiments and Size Exclusion Chromatography

In Fig. 6.11, SEC chromatograms of different eluate fractions from the column leaching test are shown. The samples were taken after elution with

1. 750 ml of demineralized water
2. 600 ml of MgSO_4 solution (0.05 mol l^{-1})
3. 800 ml of MgSO_4 solution (0.1 mol l^{-1}), and
4. 800 ml of NaOH solution (0.1 mol l^{-1})

The concentration of dissolved organic carbon (DOC) in the leachate samples was 77 mg l^{-1} (1), 12 mg l^{-1} (2), 15 mg l^{-1} (3), and 83 mg l^{-1} (4).

Elution with MgSO_4 solution led to lower DOC concentrations in the eluates compared to the elution with demineralized water. An increasing Mg^{2+} concentration obviously intensified electrostatic interactions between inorganic sediment and organic matter and

Fig. 6.10. Aggregation behavior of sediment particles in a stirring tank. Influence of MgSO_4 concentration

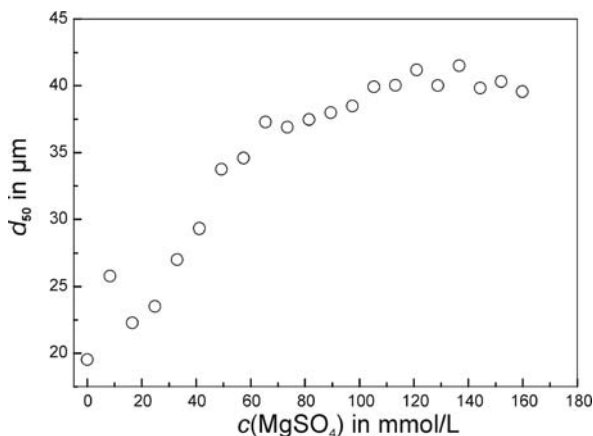
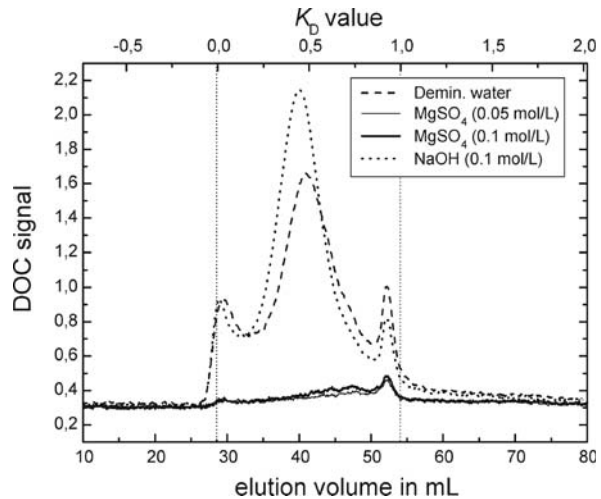


Fig. 6.11. SEC/DOC chromatograms of selected eluate fractions from the column leaching experiment



therefore, organic matter was retained in the column. Furthermore, it was noted that the availability of leachable organic matter decreased with increasing time of elution.

During elution with NaOH solution, DOC mobility increased. This was due to dissolution and release of organic matter from sediment surface.

Sorption of Heavy Metals

In the sorption experiments, the influence of organic matter on the sorption of heavy metals (Cu, Pb and Zn) onto the fine sediment particles (washed) and kaolin particles was investigated. Sediment showed a better sorption capacity for all heavy metals investigated than the kaolin (Fig. 6.12). The river sediment contained a range of different minerals (as shown in Table 6.2) with different properties and surface groups which could account for the high sorption of heavy metal cations.

Figure 6.12 shows the sorption kinetics of zinc onto sediment and kaolin in the presence and absence of organic matter. At pH 5, sorption of Zn was stronger in the absence of organic matter than in its presence. At pH 7, a positive influence of the organic matter on the zinc sorption could be determined especially in the case of kaolin. The zinc cations were probably sorbed onto the solid phase as metal-organic complexes, which are usually more stable at high pH values (Schmitt et al. 2003). The results for copper and lead which are not shown here were similar to those obtained for zinc.

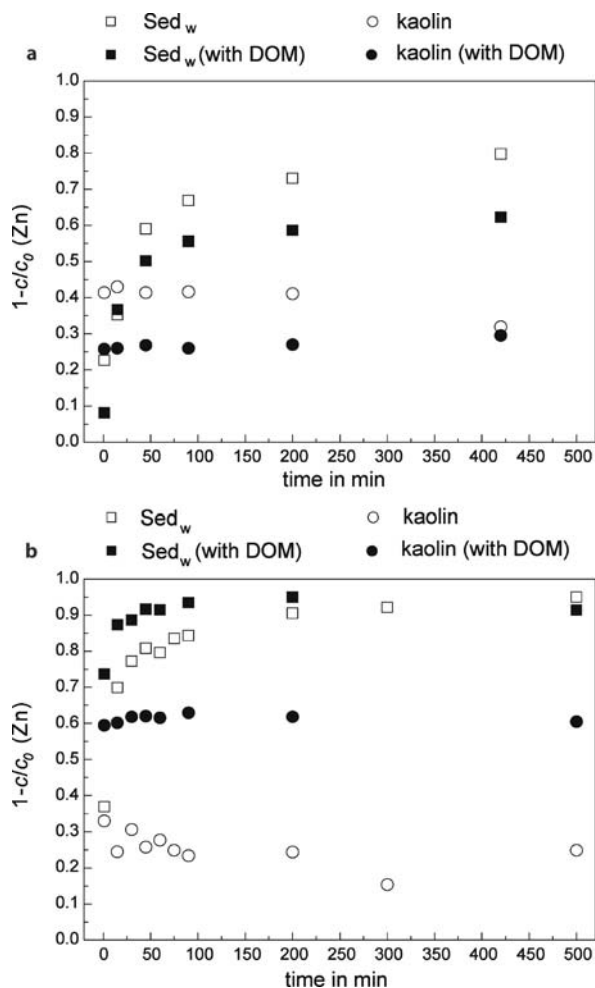
6.2.4 Conclusions

The titration and stirring tank experiments have shown that the aggregation behavior of the sediment particles is mainly influenced by the ionic strength in the aqueous phase. The pH value has little significant influence over the natural riverine range.

In rivers with low salt concentrations, it has to be expected that fine particles are stable in dispersion and thus, they remain mobile. The strong sorption of heavy metals

Fig. 6.12.

Sorption kinetics of zinc ($c_0 = 50 \mu\text{mol l}^{-1}$) onto washed sediment (Sed_w) and kaolin (concentration of the solid phases: 5 g l^{-1}) in the presence and absence of DOM (40 mg l^{-1}) at pH 5 (a) and pH 7 (b)



on the fine sediment particles can lead to an environmental risk in the context of particle mediated contaminant transport.

An increase of ionic strength (in natural systems: e.g., estuaries with mixing of river and sea water) enables particle aggregation and their sedimentation. As a consequence, contaminants would be accumulated, and stored in the river channel sediments.

Acknowledgment

The authors thank the German Ministry for Research and Education for financial support (02WF0468). The authors also thank Ulrich Reichert, Reinhard Sembritzki, and Matthias Weber for their experimental assistance. Prof. G. H. Jirka and Dipl.-Ing. G. Kühn are gratefully acknowledged for the successful cooperation.

References

- Amos CL, Grant J, Daborn DA, Black K (1992) Sea carousel – A benthic annular flume. *Estuarine, Coastal and Shelf Science* 34:557–577
- Buffle J, Leppard GG (1995a) Characterization of aquatic colloids and macromolecules. 1. Structure and behavior of colloidal material. *Environ Sci Technol* 29:2169–2175
- Buffle J, Leppard GG (1995b) Characterization of aquatic colloids and macromolecules. 2. Key role of physical structures on analytical results. *Environ Sci Technol* 29:2176–2184
- Grolimund D, Borkovec M, Barmettler K, Sticher H (1996) Colloid-facilitated transport of strongly sorbing contaminants in natural porous media: a laboratory column study. *Environ Sci Technol* 30:3118–3123
- Huber S, Frimmel FH (1992) A liquid chromatographic system with multi-detection for the direct analysis of hydrophilic organic compounds in natural waters. *Fresenius' Z Anal Chem* 342:198–200
- Kretzschmar R, Borkovec M, Grolimund D, Elimelech M (1999) Mobile subsurface colloids and their role in contaminant transport. *Advances in Agronomy* 66:121–193
- Kretzschmar R, Robarge WP, Amoozegar A (1995) Influence of natural organic matter on colloid transport through saprolite. *Water Resources Research* 31(3):435–445
- Kretzschmar R, Sticher H (1997) Transport of humic-coated iron oxide colloids in a sandy soil: influence of Ca^{2+} and trace metals. *Environ Sci Technol* 31:3497–3504
- Lick W (1982) Entrainment, deposition and transport of fine-grained sediments in lakes. *Hydrobiologica* 91:31–40
- Müller RH (1996) Zetapotential und Partikelladung in der Laborpraxis: Einführung in die Theorie, praktische Meßdurchführung, Dateninterpretation. Wissenschaftliche Verlagsgesellschaft, Stuttgart
- Roy SB, Dzombak DA (1997) Chemical factors influencing colloid-facilitated transport of contaminants in porous media. *Environ Sci Technol* 31:656–664
- Schmitt D, Saravia F, Frimmel FH, Schuessler W (2003) NOM-facilitated transport of metal ions in aquifers: importance of complex-dissociation kinetics and colloid formation. *Water Research* 37:3541–3550

Annekatriin Fritsche · Hilmar Börnick · Eckhard Worch

6.3 Equilibrium and Kinetics of Sorption/Desorption of Hydrophobic Pollutants on/from Sediments

6.3.1 Introduction

The input of anthropogenic substances into the rivers of Germany has been significantly decreased over the past few years. In contrast to the river water, sediments are still heavily polluted by metals and organic contaminants. Therefore, sediments can act as sources for contaminants. Sorption/desorption processes in the system river water/sediment are expected to be dependent on environmental conditions. But at present the knowledge regarding the effects of the hydrochemical and hydrodynamical conditions on remobilization of pollutants out of historical contaminated sediments is still insufficient.

The objectives of this work were to investigate the effect of dissolved natural organic matter (DOM) onto sorption and desorption processes and competition effects among hydrophobic organic contaminants (HOC). Furthermore, sorption and desorption processes of HOCs were investigated under different hydrodynamic conditions.

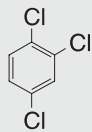
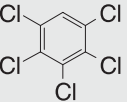
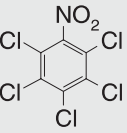
6.3.2 Experimental Methods

Sediment materials and water. Natural river sediment, taken out of an old anabranch of the river Elbe near Torgau/Germany, was used for the study. As a pretreatment step, the sediment, containing an organic fraction of 0.24% ($f_{OC} = 0.0024 \text{ g g}^{-1}$ dry weight), was dried at 40 °C, sieved (<2 mm) and homogenized. The experiments were accomplished with natural water possessing different concentrations and consistence of natural DOM (laboratory water: about 1 mg l^{-1} , river water: 6 mg l^{-1} , pond water: 14 mg l^{-1}). The ionic strength of the pond and river water was about $400 \mu\text{S cm}^{-1}$. Sodium chloride was added to the laboratory water to set its ionic strength to an equal level as pond and river water. Preliminary analysis of all water and sediment materials used in the study showed no contamination with the model pollutants.

Chemicals. For the investigations three relevant anthropogenic compounds were selected: 1,2,4-trichlorobenzene, pentachlorobenzene and pentachloronitrobenzene (PESTANAL®, purchased from Riedel-de Haën). The criteria of substance selection were their appearance in the list of priority pollutants of the EU (directive 2000/60/EC), their occurrence in rivers, and their biological and chemical persistence within the experimental periods. The structure, aqueous solubility and octanol-water partitioning coefficients (K_{OW}) of the model compounds are shown in Table 6.3.

Experimental methods. All experiments were performed in the dark, in completely mixed batch (CMB) reactors, with equal solid-to-water ratios (10 g dry sediment, 200 ml solution). Within the sorption experiments, the concentration of each investigated model contaminant was in a range of 2 to $500 \mu\text{g l}^{-1}$. The CMB reactors were shaken for sorp-

Table 6.3. Structure and properties of investigated model contaminants (Chemical Fact Sheet 2005)

	Structure	Aqueous solubility S (mg l^{-1} , 20 °C)	$\log K_{OW}$
1,2,4-Trichlorobenzene		49	3.8 ... 4.2
Pentachlorobenzene		0.5	4.8 ... 5.4
Pentachloronitrobenzene		0.8	4.2 ... 4.8

tion equilibration. The desorption experiments were done by replacing the supernatant liquid phase with contaminant-free water after the sorption experiments. Afterwards, the CMB reactors were shaken until a state of desorption equilibrium was reached.

Desorption kinetics were studied using equally preloaded sediment. For preloading 200 g dry sediment and 300 ml liquid phase containing $500 \mu\text{g l}^{-1}$ of each model contaminant were shaken for 170 h reaching the state of sorption equilibrium. Afterwards, the supernatant liquid was decanted off. Desorption experiments were performed with 10 g of the preloaded solid phase and 200 ml contaminant-free water. To determine the increase of liquid-phase concentration during the desorption process, samples were taken after different times. For the investigation of the effect of hydrodynamical conditions on the desorption process, the agitation within the CMB-reactors was varied (0, 100, 150 and 200 rotations per minute).

All experiments were replicated at least twice. The errors including analytical and methodical deviation are about 10% for sorption and up to 23% for desorption equilibrium experiments. The error of kinetic experiments are up to 50%.

Analytical methods. Prior to analysis, the model contaminants were separated from the aqueous phase by liquid-liquid extraction with dichloromethane. Therefor, 50 ml liquid phase, 5 g sodium chloride and 3 ml dichloromethane were shaken for 45 min at 250 rpm. The organic phase was isolated and dried with sodium sulfate. The solid samples were extracted with a mixed solvent consisting of acetone and dichloromethane (1:4 vol:vol). The extracts were concentrated in a rotary evaporator, dried and cleaned in sodium sulfate/Florisil®-cartridges and concentrated to 1 ml in a gentle stream of nitrogen. The analysis of liquid phase and sediment extracts were accomplished in a GC-MS system (Thermo Quadrupol MS Trace DSQ). 1,2,3,4-Tetrachloro-5-nitrobenzene and 1,3,5-tribromobenzene were used as internal standards.

The organic content of solid phases was analyzed by a TOC-Analyser with boat sampler (Rosemount Analytical Dohrmann DC-190) after digestion with hydrochloric acid. The DOM content of the liquid phase was analyzed by a Shimadzu TOC-5000-Analyser and quantified as non-purgeable organic carbon (NPOC). Since volatile organic compounds are not relevant for the investigated water samples, NPOC can be set equal to DOC (dissolved organic carbon).

6.3.3 Results and Discussion

Equilibrium Experiments

To investigate a possible *competition effect among the model contaminants*, isotherms were determined by using single contaminant/DOM and mixed contaminants/DOM systems. The mixed system contained respectively 2 to $500 \mu\text{g l}^{-1}$ of 1,2,4-trichlorobenzene, pentachlorobenzene and pentachloronitrobenzene in addition to the natural DOM. For this purpose, river Elbe water was used as liquid matrix. The sorption coefficients were acquired from the first linear part of the isotherms and normalized to the organic carbon content of the solid phase ($f_{\text{OC}} = 0.0024 \text{ g g}^{-1}$ dry weight). In Table 6.4, the results of the single contaminant and mixed contaminant sorption isotherms are shown.

Table 6.4. Competition effect – partitioning coefficients of the sorption isotherms

	$\log K_{OC}$ (single contaminant/DOM)	$\log K_{OC}$ (mixed contaminants/DOM)	$\log K_{OC}$ (literature)
1,2,4-Trichlorobenzene	3.5	3.8	3.8 ... 4.2
Pentachlorobenzene	4.1	4.7	4.8 ... 5.4
Pentachloronitrobenzene	4.3	4.8	4.2 ... 4.8

Table 6.5.

Results of the sorption and desorption isotherms in dependence on the DOM concentration in the liquid phase

	DOC (water) (mg l^{-1})	$\log K_{OC, \text{Sorption}}$ (mixed contaminants/DOM)	$\log K_{OC, \text{Desorption}}$ (mixed contaminants/DOM)
1,2,4-Trichlorobenzene	1	3.7	4.4
	6	3.8	4.2
	14	3.7	4.3
Pentachlorobenzene	1	4.5	5.0
	6	4.7	4.9
	14	4.7	4.9
Pentachloronitrobenzene	1	4.4	5.2
	6	4.8	5.1
	14	4.5	5.2

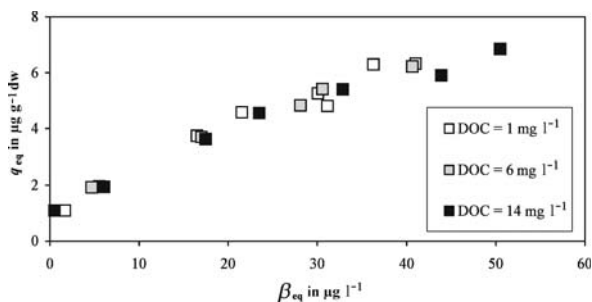
No significant competition effects among the investigated model contaminants could be observed for sorption or for desorption processes.

Additional to the competition effect, the *influence of the DOM concentration on the sorption and desorption* was investigated. During the river Elbe flood in 2002, an obvious increase of the dissolved organic carbon (DOC) concentration of the river water was detected (Börnack et al. 2003). According to several authors (e.g., Chiou et al. 1986; Laor et al. 1998), the sorption processes of HOCs is influenced by DOM. Amiri et al. (2005) showed that sorption of nitro-substituted organic compounds was significantly influenced by the DOC content of the liquid phase. In column experiments, Reemtsma et al. (2003) found a linear correlation between the mobility of adsorbable organic halogen compounds and the release of solid organic matter connected with increasing DOC concentrations. The sorption of 1,2,4-trichlorobenzene, pentachlorobenzene and pentachloronitrobenzene was not influenced by the concentration of DOM (Table 6.5). The results of desorption isotherms with different DOM concentration in the liquid phase showed no influence of DOM on the desorption process of the investigated HOCs (Fig. 6.13, Table 6.5).

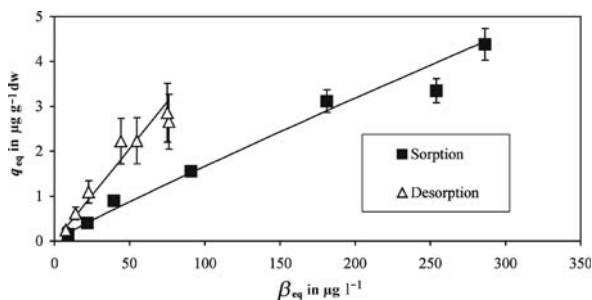
For all compounds investigated, there is an obvious discrepancy between the partitioning coefficients calculated from the sorption and desorption data. The comparison in Table 6.5 indicates that the partitioning coefficients of desorption isotherms are above the results of the sorption isotherms. The so-called hysteresis effect could be assumed to be the reason for this effect. The differences between sorption and desorption isotherms can be seen in Fig. 6.14. According to literature (Pignatello 2000), hysteresis can be explained by (a) an inadequate time allowed for equilibration or (b) by

Fig. 6.13.

Desorption isotherms of pentachlorobenzene in water possessing different amounts of DOM (quantified as DOC). q_{eq} : equilibrium loading of sediment; β_{eq} : equilibrium concentration in the aqueous phase

**Fig. 6.14.**

Comparison of sorption and desorption isotherms of 1,2,4-trichlorobenzene in river Elbe water



the occurrence of irreversibly or resistantly sorbed fractions. Case (a) can be excluded because sorption kinetic experiments showed that the systems under consideration reached equilibrium after three days (see kinetic curves in the following section) while the duration of each sorption isotherm experiment was seven days. Furthermore, long-term kinetic tests with duration of four weeks resulted in the same loading of the investigated contaminants on the sediment as the experiments with duration of only three days. Therefore, the observed discrepancy between sorption and desorption isotherms as presented in Fig. 6.14 must be caused by a resistantly sorbed fraction, characterized by very slow desorption kinetics, or irreversibly sorbed fractions (case (b)).

Desorption Kinetics

The aims of kinetic experiments were to get information about the influence of DOM and hydrodynamic conditions on the rate and extent of HOC remobilization out of contaminated river sediments. The experiments were conducted with sediments equally preloaded with model compounds. The results were analyzed using an overall kinetic model based on the following equation:

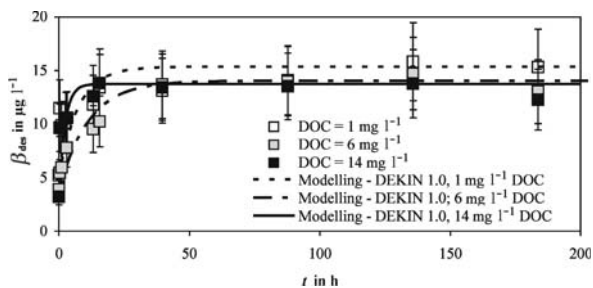
$$\frac{dq}{dt} = -k_{des}(q - q^*)$$

with q : loading of sediment at time t , k_{des} : desorption rate constant, q^* : equilibrium loading of sediment at time t .

The desorption rate constants were estimated by curve fitting using the program DEKIN 1.0. The highest measured standard deviation of the desorption rate constant

Fig. 6.15.

Desorption kinetics of 1,2,4-trichlorobenzene in water possessing different DOM concentrations in a strongly resuspended system

**Table 6.6.**

Desorption rate constants of investigated HOCs for different DOM concentrations in a non-resuspended system

DOC (mg l ⁻¹)	k_{des} (1,2,4-trichlorobenzene) (s ⁻¹)	k_{des} (pentachlorobenzene) (s ⁻¹)	k_{des} (pentachloronitrobenzene) (s ⁻¹)
1	3.6×10^{-6}	7.6×10^{-8}	2.5×10^{-6}
6	2.6×10^{-6}	8.0×10^{-8}	3.0×10^{-6}
14	3.0×10^{-6}	15.0×10^{-8}	1.3×10^{-6}

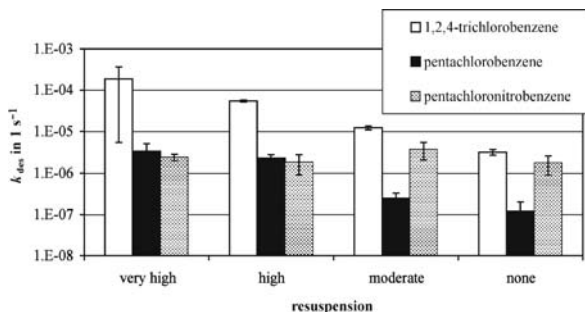
within the desorption kinetic experiments were $0.9 \times 10^{-6} \text{ s}^{-1}$ for 1,2,4-trichlorobenzene, $5.0 \times 10^{-8} \text{ s}^{-1}$ for pentachlorobenzene and $0.9 \times 10^{-6} \text{ s}^{-1}$ for pentachloronitrobenzene. Taking in account these standard deviations it can be concluded, that the desorption experiments showed no significant differences in the kinetic curves (Fig. 6.15) and in the desorption rate constants (Table 6.6) determined for different DOM concentrations. It can be derived from these experiments that there is no influence of the DOM concentration on the remobilization rate of the investigated HOCs for all investigated hydrodynamic conditions.

To investigate the influences of the hydrodynamic conditions on the desorption process the CMB-reactors were exposed to different agitation rates. As can be seen in Fig. 6.16, the desorption rate constants, k_{des} , of pentachlorobenzene and 1,2,4-trichlorobenzene were strongly controlled by the intensity of resuspension within the system. For pentachloronitrobenzene desorption, no obvious impact of the hydrodynamic conditions was noticed. It seems that the influence of hydrodynamics on the desorption rate constant is specific for each substance. This is in accordance with findings of Latimer et al. (1999) who showed for polycyclic aromatic hydrocarbons that remobilization depends on the chemical properties of the adsorbed substance.

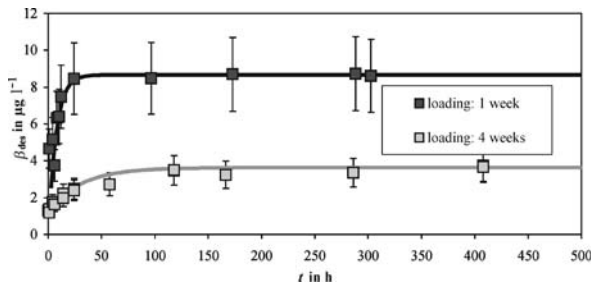
In contrast to the desorption rates, the equilibrium concentrations of the model contaminants after desorption were not influenced by the hydrodynamic conditions. On the other hand, there was a strong impact of the liquid-solid contact time during preloading on the desorption equilibrium concentration indicating an increase of sorption strength with time. In Fig. 6.17, the kinetic curves of 1,2,4-trichlorobenzene desorption after HOC/sediment contact times of one and four weeks are shown for a moderately resuspended system. Although the mass sorbed onto the sediment was nearly the same in both cases ($0.22 \mu\text{g g}^{-1}$ vs. $0.21 \mu\text{g g}^{-1}$), the desorption after a preloading time of four weeks was much lower than the desorption after one week preloading time. Experiments in a non-resuspended system showed that the desorp-

Fig. 6.16.

Effect of hydrodynamic conditions on the desorption rate constant, k_{des}

**Fig. 6.17.**

Influence of the HOC/sediment preloading contact time on the desorption process of 1,2,4-trichlorobenzene in a moderately resuspended system



tion of pentachlorobenzene and pentachloronitrobenzene also decreases with preloading time. After a preloading time of 20 days 30% of the sorbed 1,2,4-trichlorobenzene, 14% of pentachlorobenzene and 34% of pentachloronitrobenzene were desorbed. The increasing of preloading time up to 32 days, decreased the reversibly sorbed fractions to 26% for 1,2,4-trichlorobenzene, 4% for pentachlorobenzene and 11% for pentachloronitrobenzene. Since it is known that the investigated HOCs are biodegradable under anaerobic conditions, the experiments were performed under aerobic conditions. Thus, the determined effect could be explained by a change of the ratio of reversibly and irreversibly/resistantly sorbed fractions, which was already described in the discussion of sorption and desorption isotherms (Fig. 6.13). In the literature, this effect is referred to as “aging” (Alexander 2000; Reid et al. 2000; Lee et al. 2004) and is caused by diffusion of molecules into deeper layers of the sorbent particles, whereby the bioavailability of the HOCs and the possibility of remobilization of contaminants out of polluted sediments decreases. On the other hand it is possible that changes in hydrodynamic or in hydrochemical conditions can remobilize HOCs also from historical contaminated sediments (Alexander, 2000).

Taking into account the standard deviations given before, it can be stated that the desorption rate constants were not significantly influenced by the HOC/sediment preloading contact time. It can be assumed that the values of k_{des} given in Table 6.7 represent only the fast desorbing fractions that are not influenced by the HOC/sediment contact time. The run-times of the experiments (up to 400 h) were not long enough to find out if there is an additional slow desorption step, as postulated by Cornelissen et al. (1997). Long-term experiments of about a half year would be necessary to decide if there is a resistant, characterized by a very slow desorption, or an irreversible sorption.

Table 6.7.
Desorption rate constants of the model contaminants against sediment/HOC contact time in a non-resuspended system

HOC/sedi- ment contact time t (d)	k_{des} (1,2,4-trichlo- robenzene) (s^{-1})	k_{des} (pentachloro- benzene) (s^{-1})	k_{des} (pentachloro- nitrobenzene) (s^{-1})
17	2.7×10^{-6}	8.0×10^{-8}	3.2×10^{-6}
20	3.8×10^{-6}	19.5×10^{-8}	1.0×10^{-6}
32	2.9×10^{-6}	7.2×10^{-8}	1.8×10^{-6}

6.3.4 Conclusions

In contrast to statements in literature for other HOCs, our results showed that sorption and desorption processes of 1,2,4-trichlorobenzene, pentachlorobenzene and pentachloronitrobenzene were not influenced by the DOM concentration in the investigated range from 1 to 14 mg l⁻¹ DOC. However, an effect of the hydrodynamic conditions and the HOC/sediment contact time on the desorption process was observed. Higher resuspension rates increased the desorption rate constant of chlorinated aromatic hydrocarbons, whereas the release of pentachloronitrobenzene was not affected by different strength of agitation. Therefore, the remobilization of HOCs out of contaminated sediments seems to be a function of chemical properties. For a better understanding of the influence of chemical properties on the extent of contaminant remobilization further research is needed.

The sorption of the investigated model contaminants was not completely reversible, which might be caused by resistantly and irreversibly sorbed fractions. The resistantly and irreversibly sorbed fractions increased with time (“aging effect”). It can be concluded from our results, that the possibility of remobilization of the investigated contaminants out of polluted sediments decreases with time.

References

- Alexander M (2000) Aging, bioavailability and overestimation of risk from environmental pollutants. *Environmental Science and Technology* 29:2713–2717
- Amiri F, Börnick H, Worch E (2005) Sorption of phenols onto sandy aquifer material: the effect of dissolved organic matter (DOM). *Water Research* 39:933–941
- Börnick H, Grischek T, Worch E (2003) Ausgewählte Untersuchungsergebnisse von Wasser- und Schlammproben aus dem Raum Dresden während des Elbe-Hochwassers im August 2002. Proc. Jahrestagung der Wasserchemischen Gesellschaft, Stade, pp 211–217
- Chemical Fact Sheet (2005) www.speclab.com/compound/chemabc.htm
- Chiou CT, Malcolm RT, Brinton TI, Klie DE (1986) Water solubility enhancement of some organic pollutants and pesticides by dissolved humic and fulvic acids. *Environmental Science and Technology* 37:5657–5664
- Cornelissen G, van Noort PCM, Govers HAJ (1997) Desorption kinetics of chlorobenzenes, polycyclic aromatic hydrocarbons, and polychlorinated biphenyls: Sediment extraction with Tenax(R) and effects of contact time and solute hydrophobicity. *Environmental Toxicology and Chemistry* 16:1351–1357
- Directive 2000/60/EC of the European Parliament establishing a framework for community action in the field of water policy (2000)
- Laor Y, Farmer WJ, Aochi Y, Strom P (1998) Phenanthrene binding and sorption to dissolved and to mineral-associated humic acid. *Water Research* 32:1923–1931

- Latimer JS, Davis WR, Keith DJ (1999) Mobilization of PAHs and PCBs from in-place contaminated marine sediments during simulated resuspension events. *Estuarine, Coastal and Shelf Science* 49:577–595
- Lee S, Kommalapati RR, Valsaraj KT, Pardue JH, Constant WD (2004) Bioavailability of reversibly sorbed and desorption-resistant 1,3-dichlorobenzene from a Louisiana superfund site soil. *Water, Air and Soil Pollution* 158:207–221
- Pignatello JJ (2000) The measurement and interpretation of sorption and desorption rates for organic compounds in soil media. *Advances in Agronomy* 69:1–73
- Reemtsma T, Savric I, Jekel M (2003) A potential link between the turnover of soil organic matter and the release of aged organic contaminants. *Environmental Toxicology and Chemistry* 22:760–766
- Reid BJ, Jones KC, Semple KT (2000) Bioavailability of persistent organic pollutants in soils and sediments – a perspective on mechanisms, consequences and assessment. *Environmental Pollution* 108:103–112

Andreas Kleeberg · Michael Hupfer · Giselher Gust

6.4 Phosphorus Entrainment Due to Resuspension, River Spree, NE Germany

6.4.1 Introduction

Both resuspension and transport of suspended particulate matter (SPM) are driven largely by hydrodynamics at the sediment water interface, initiating and controlling the particle exchange between river sediment and water column (e.g., Black et al. 2002; El Ganaoui et al. 2004). Transport of suspended sediment is accompanied by the transport of phosphorus (P). It is an important mechanism to understand as the transport of sediment-associated P in lowland rivers often constitutes a high percentage (23–61%) of the total annual P load (e.g., Svendsen et al. 1995). Interactions of resuspended SPM and particulate P require knowledge of sediment properties and hydrodynamic conditions, such as the composition, the critical shear stress, the entrainment rate as well as the sinking velocity (El Ganaoui et al. 2004). They are often inferred through the use of flume experiments (Redondo et al. 2001; Witt and Westrich 2003; El Ganaoui et al. 2004) or from direct in situ measurements (Gust and Morris 1989; Black et al. 2002). For rivers, the availability of fine-grained sediments on the stream bed is viewed as a transient depositional feature (e.g., Droppo and Stone 1994; Bungartz and Wanner 2004). This paper reports on an in situ experiment on river bed resuspension in a stretch of lowland river Spree in comparison to a concurrent laboratory experiment. The aim of this study is to (1) determine erosion thresholds of sediments and benthic particulate P, (2) determine entrainment rates, and (3) address problems in applying results from laboratory experiments to riverine conditions.

6.4.2 Material and Methods

Study Site

River Spree, NE Germany, is a medium-sized lowland river with a catchment area of about 10 000 km². The river emerges at an elevation of 580 m, and flows for 400 km to Berlin through several shallow lakes affected by river regulation (Köhler et al. 2002; Bungartz and Wanner 2004). The experimental site Kossenblatt (14° E, 52°07' N) is

part of a 21.1 km long sixth-order section of the river and represents a slow flowing ($0.1\text{--}0.3\text{ m s}^{-1}$) stretch of the Krumme Spree. The slope of the trapezoid profile is 0.01%, and the runoff (Q) usually varies between 12 and $16\text{ m}^3\text{ s}^{-1}$ at water depths of $1.5\text{--}2.5\text{ m}$ (Bungartz and Wanner 2004).

Methods

In both the in situ and the laboratory experiments, an erosion chamber (Gust 1990), hereafter called microcosm MC, with spatially homogeneous bottom stress τ , has been used (Fig. 6.18). Calibration of shear velocity u^* ($= (\tau/\rho)^{1/2}$, ρ = density) of the MC has been conducted using a variety of approaches (Gust 1990; Gust and Müller 1997; Tengberg et al. 2004).

For the in situ experiment (INS), on 19 May 2005, the MC (i.d. 19.2 cm) was deployed by means of a tripod. A scuba diver adjusted the distance between stirring disk and sediment surface (8 cm). Required river water feed through was provided continuously by a peristaltic pump at $Q = 245 \pm 1\text{ ml min}^{-1}$.

For the laboratory experiment (LAB), on 31 May 2005, 20 undisturbed sediment cores taken with a sediment corer (UWITEC[®], Mondsee, Austria) were sliced in the field down-core into two horizons (0–3, 3–8 cm), pooled and placed stratified into the MC. The MC was gently filled with $\sim 4\text{ l}$ unfiltered Spree water and kept for 12 days in the dark at room temperature for consolidation and conditioning, respectively.

In the two runs of the experiment INS and LAB u^* ranged from 0.57 to 1.67 cm s^{-1} . It was incrementally increased every 20 minutes (see Fig. 6.19). Data on turbidity were recorded continuously (0.1 min^{-1}) by a commercial Forward Scatter Turbidimeter TF

Fig. 6.18.

Experimental arrangement for the in situ determination of entrainment rates due to resuspension. The microcosm was driven as an open system. For the laboratory experiments a closed microcosm with a reservoir supplying continuously river water was used instead of the open river inflow

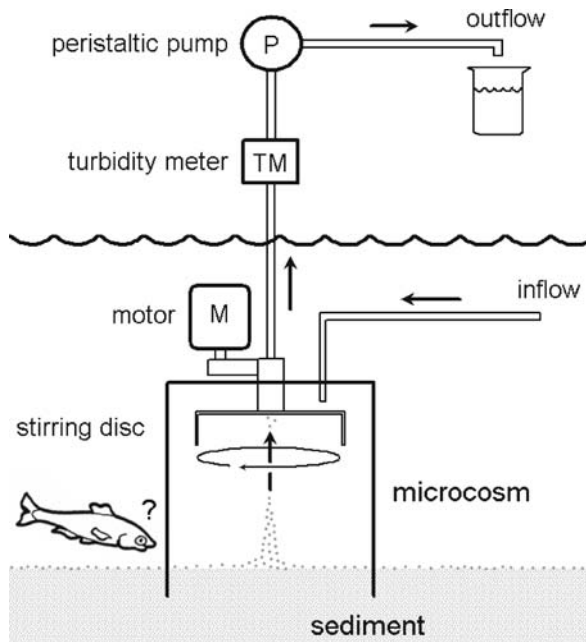
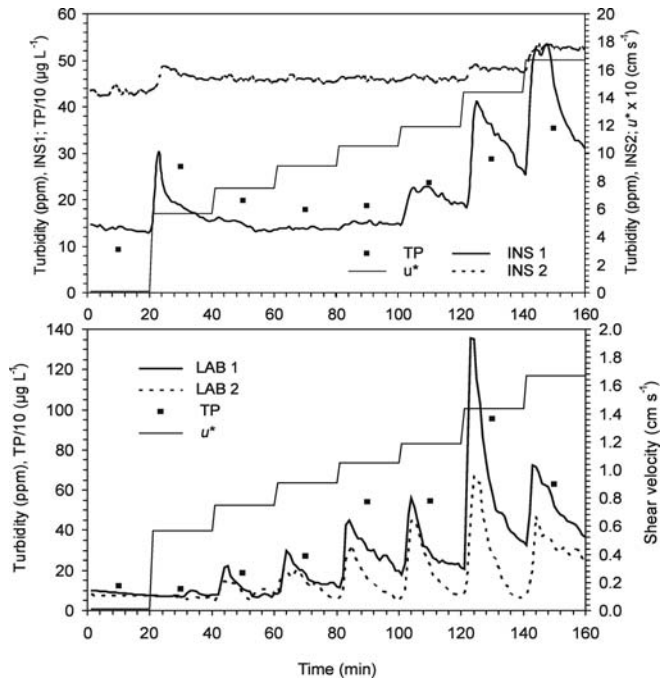


Fig. 6.19.

Course of turbidity for the first (INS 1) and second run (INS 2) of the in situ experiment at Kossenblatt, 19 May 2005 (*upper panel*), and for the first (LAB 1) and second run (LAB 2) of the repetition of the in situ experiment under laboratory conditions, 31 May 2005 (*lower panel*) at an incrementally enhanced shear velocity (u^*). The changing concentration of total P (TP) is plotted for INS 1 and LAB 1. Note that in INS u^* was multiplied by 10, and TP divided by 10, and in LAB TP divided by 10



10-512 (Optek-Danulat, Essen 1, Germany) with Labview®. An integrated water sample for chemical analysis was taken for each u^* interval. SPM was determined in triplicate by filtering water samples through pre-weighed cellulose acetate filters (0.45 µm, Sartorius, Göttingen, Germany), drying at 105 °C, and weighing again. Means of turbidity ($n = 10$) provided the calibration curve for SPM (mg l⁻¹) with (ppm) $\times \sim 1.5 =$ (mg l⁻¹). 50 ml suspension aliquots of LAB 1 were taken at selected u^* to determine the sinking velocity spectra of the resuspended particles. By pipetting 0.65 ml subsamples into a settling column of 50 mm i.d. and 600 mm length, sinking velocity w_s of particle ensembles from $u^* = 0, 0.85$ and 1.44 cm s⁻¹ were filmed by a video camera (Sony DCR-PC110E PAL) and subsequently processed by MATLAB software (Version 2006a) providing in addition to spectra of w_s and aggregate size other derived variables utilizing Stoke's Law. For the statistical treatment 14 commensurate w_s classes from 50 to 400 m d⁻¹ with 25 m d⁻¹ each were used.

Soluble reactive P (SRP) was determined photometrically (Murphy and Riley 1962) using a segmented flow analyzer (Skalar San^{plus}). Total P (TP) in water samples was measured as SRP after wet digestion using peroxodisulfate for 2 h at 121 °C and 0.12 MPa. Total iron (TFe) concentration was analyzed with a flame atomic absorption spectrometer (Perkin Elmer 3300, Rodgau-Juegesheim) after aqua regia digestion.

To study the P distribution for particles size classes and sinking behavior a step-wise filtration scheme following Shand et al. (2000) was carried out. Four glass settling tubes (i.d. 4.7 cm, height 30 cm) were filled with river water from four sampling stations near Kossenblatt (Radinkendorf, 27/28 April 2005) and stored vertically in a large container filled with river water (for details see Bungartz and Wannner 2004). Upper-

most 435 ml water were withdrawn at 0 h, after 1, 6, and 24 h. TP and TFe were determined from an unfiltered aliquot. TP was also determined in filtrates after a step-wise filtration with 1 μm (PC, Whatman), 0.8 μm (PC, Whatman), 0.45 μm (CA, Schleicher and Schuell), and 0.2 μm (CA, Whatman) membrane filters giving total dissolved P (DTP). Particulate P (PP) is the difference between TP and DTP.

Calculations

Since the MC was driven as an open system in INS and LAB, entrainment rates (E) per step (x) of u^* were calculated in terms of a mass balance as follows:

$$E_x = \sum_{i=1}^n \left(\frac{L_{x\text{out}} - L_{x\text{in}}}{A} \right) \quad (\text{mg m}^{-2} \text{ h}^{-1}) \quad (6.2)$$

where L_x is the load of x at the outflow (out) and inflow (in) (mg h^{-1}) and A is the area of the MC (0.037 m^2). The individual L_x in Eq. 6.2 was calculated by multiplying the concentration of x (mg m^{-3}) and the water discharge of the peristaltic pump ($\text{m}^3 \text{ h}^{-1}$). The period of time within the amount of sedimentary resuspendable matter has been exhausted for a given u^* was calculated from the time difference from when the concentration of SPM was at maximum and the beginning of the respective stepwise increase in u^* . The theoretical particle transport distance was calculated according to Thomas et al. (2001).

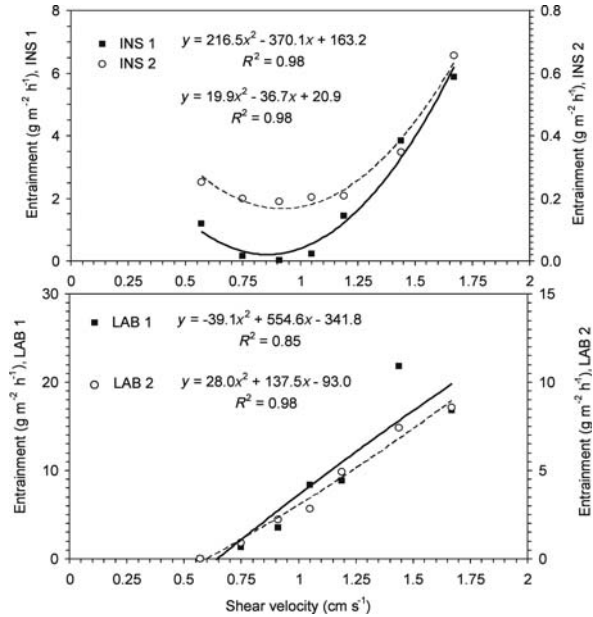
6.4.3 Results

In the first run of the in situ experiment (INS 1) there was a remarkable turbidity peak at the beginning of the first step of u^* (0.57 cm s^{-1}). This yielded an entrainment rate of $1.177 \text{ mg m}^{-2} \text{ h}^{-1}$, equal to the amount of SPM (9.2% of total SPM) generated in the fifth step of u^* (1.19 cm s^{-1}) with 11.3% of total SPM of this run (Fig. 6.19, upper panel). Located only about 1 m adjacent to the first site (INS 1), the sediments of the second in situ run (INS 2) revealed large differences in all parameters determined, yet with a similar trend in the entrainment curve. The first peak in INS 2 at $u^* = 0.57 \text{ cm s}^{-1}$ is identical, but at a much lower entrainment rate ($251 \text{ mg m}^{-2} \text{ h}^{-1}$). It provided approximately the same proportion of SPM (12.3% of total SPM) as at the fifth step of u^* (1.19 cm s^{-1}) with 10.1% of total SPM. The stock of easily resuspendable matter forming surface sediments was exhausted after 9 min (INS 2) and 11 min (INS 1), respectively. The time series of TP were identical in their major trend in both experimental cases, except that the concentration in LAB 1 was higher by a factor of two than in INS 1. The fraction of particulate P in River Spree inflow water at Kossenblatt amounted to 74.5% TP. In the course of INS this ratio remained relatively constant, i.e. $66.5 \pm 7.9\%$ TP in INS 1 and $67.2 \pm 7.9\%$ TP in INS 2.

In contrast to the INS runs, no peak in turbidity arose in the laboratory (LAB) runs at the lowest u^* , indicating the absence of flocculent, easily resuspendable material at the sediment surface (Fig. 6.19, lower panel). The subsequent time series of turbidity under incremental increases of u^* was similar except for the maximum peak of LAB 1 at $u^* 1.44 \text{ cm s}^{-1}$. For both experimental cases the peak always coincided with the highest

Fig. 6.20.

Entrainment rates (SPM dry weight) vs. shear velocity for the in situ experiment (INS, upper panel), and the laboratory experiment (LAB, lower panel)



concentration of TP. The fraction of particulate P in inflowing river water was only 21.8% TP as a result of fast particle settling in the reservoir. In comparison, particulate P averaged $79.9 \pm 14.2\%$ in INS 1 and $85.0 \pm 9.9\%$ in INS 2.

In the experiment LAB, an analog major increase of entrainment with an increasing u^* is found (Fig. 6.20). The entrainment rates of LAB 1 are about two times higher than those of LAB 2, indicating a reduced heterogeneity compared to the INS data since aliquots from a pooled sediment sample are used. The shape of the best fit, almost a straight line, illustrates the absence of easily resuspendable matter at low u^* .

Phosphorus entrainment rates also increased with an increasing u^* ; those of INS 1 and INS 2 differed by a factor of approx. 6, and those of LAB 1 and LAB 2 by a factor of 1.5 (Fig. 6.21).

The mean values of particle parameters (Table 6.8) did not change significantly with increasing u^* (Fig. 6.19, LAB 1). In the w_s frequency distribution the percentage of particle number was constant with increasing u^* . Whereas, in the particle masses the percentage of light particles in the fractions with lower w_s ($75\text{--}200$ m d⁻¹, $n = 6$ w_s classes) decreased from 94.9% at $u^* = 0$ cm s⁻¹, to 86.3% at $u^* = 0.85$ cm s⁻¹, and to 74.3% at $u^* = 1.44$ cm s⁻¹. Inversely, the percentage of heavier particles in the fractions with higher w_s ($275\text{--}400$ m d⁻¹, $n = 6$ w_s classes) increased from 3.3% at $u^* = 0$ cm s⁻¹, to 4.9% at $u^* = 0.85$ cm s⁻¹, and to 17.9% at $u^* = 1.44$ cm s⁻¹.

The eroded particles, represented as SPM from experiments LAB with their relatively high w_s (Table 6.8) cannot move downstream very far prior to subsequent resuspension (Fig. 6.22). For example particles with a w_s of 225 m d⁻¹ would be transported over 200 m. Since preferentially particles with a higher w_s were resuspended at $u^* = 1.44$ cm s⁻¹ the higher SPM concentration compared to that at $u^* = 0.85$ cm s⁻¹ decreases faster towards the level of the river Spree water.

Fig. 6.21. Phosphorus entrainment rates vs. shear velocity for the in situ experiment (INS, upper panel), and the laboratory experiment (LAB, lower panel)

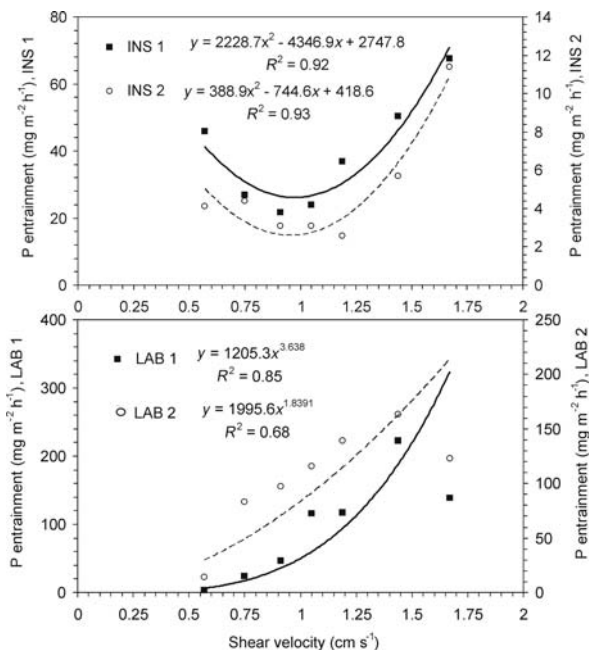


Table 6.8. Mean values ± standard deviation for characteristics of particles resuspended in the first laboratory run (see Fig. 6.18, LAB 1) at an increasing shear velocity

Particle parameter	Unit	Shear velocity (cm s ⁻¹)		
		0	0.85	1.44
Number		497	11 010	1 454
Sinking velocity	m d ⁻¹	113.0 ± 37.7	114.5 ± 53.6	112.6 ± 41.6
Area	mm ²	0.023 ± 0.03	0.016 ± 0.01	0.026 ± 0.05
Diameter ^a	µm	134.3 ± 71.7	119.2 ± 42.9	133.4 ± 81.2
Mass ^a	mg	2.8 ± 5.5	1.4 ± 2.1	3.6 ± 13.1
Density ^a	g cm ⁻³	1.154 ± 0.09	1.151 ± 0.08	1.149 ± 0.09

^a Calculated from Stoke's law.

As a result of the enhancement of SPM concentration (Fig. 6.22) at an u^* of 0.85 and 1.44 cm s⁻¹ the in situ TP concentration of river Spree would theoretically enhance from 122 µg l⁻¹ by 6 and 36 µg l⁻¹, respectively.

The stepwise filtration reveals that most P (62.9 ± 16.6%, $n = 12$) is associated with larger particles (>1 µm) representing the 'coarse particulate P' (Fig. 6.23) which is settling relatively fast. TP decreased at decreasing rates of P sedimentation from 3.68 mg m⁻² h⁻¹ (after 1 h), to 0.54 mg m⁻² h⁻¹ (after 6 h), and 0.17 mg m⁻² h⁻¹ (after 24 h). The same applies to TFe (Fig. 6.23). The percentage of 'coarse particulate P' (>1 µm) in the sus-

Fig. 6.22.

Theoretical particle transport distance for 15 commensurate groups of a sinking velocity spectrum at $u^* = 1.34 \text{ cm s}^{-1}$ from LAB 1 (Tab. 6.8) and the decrease of suspended particulate matter (SPM) concentration after a resuspension event in the water column of river Spree (discharge = $16 \text{ m}^3 \text{ s}^{-1}$) back towards the initial SPM concentration of 13.14 mg l^{-1}

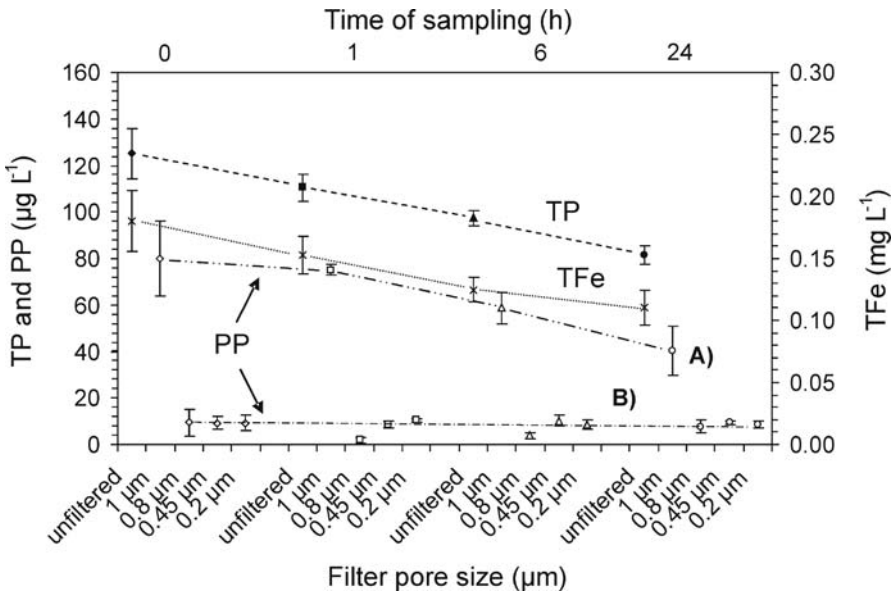
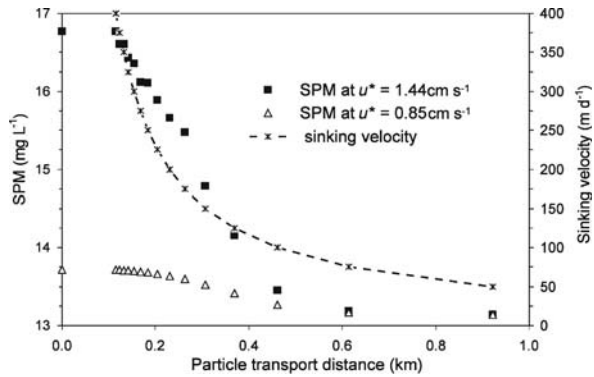


Fig. 6.23. Results from a step-wise filtration of a water sample taken after 0, 1, 6 and 24 h out of settling tubes. Since the fractional P distributions among the four sampling stations of river Spree (Radinkendorf, 27/28 April 2005) did not significantly differ, means and standard deviations of $n = 4$ are shown. Filled symbols represent total P (TP), cross symbols total Fe (TFe), and open symbols particulate P (PP). PP fractions are operationally defined as follows: $>1 \mu\text{m}$ = 'coarse particulate P' (case A), $<1 \dots >0.8 \mu\text{m}$ = 'fine particulate P', $<0.8 \dots >0.45 \mu\text{m}$ = 'coarse colloidal P', $<0.45 \dots >0.2 \mu\text{m}$ = 'fine colloidal P' (case B). Phosphorus $<0.2 \mu\text{m}$ = 'dissolved P'

pendent flocs decreased within 24 h down to $49.3 \pm 12.9\%$ (case A). Theoretically, the smaller the particle size in the filtrate the smaller the PP concentration and the slower its decrease. However, there were no changes in the concentration from the 0 h to the 24 h sample of the 'fine particulate P' (16.9–16.1%), the 'coarse colloidal P' (23.7–27.6%) as well as the 'fine colloidal P' (34.5–35.7%) which remained on the same level (case B). The dissolved P ($<0.2 \mu\text{m}$, not shown) was only 5.9 to 10.2% of TP.

6.4.4 Discussion

Besides the great variability in the time series and rates within both runs of INS and LAB experiments (Fig. 6.19), comparison reveals that entrainment of sediment and associated P is controlled by u^* (Figs. 6.20 and 6.21) as well as sediment heterogeneity and consolidation depending on river bed conditions. Run INS 1 confirms the existence of a fine-grained fluffy layer at the sediment surface with high water contents easily eroded, with a low critical u^* threshold for resuspension (e.g., Droppo and Stone 1994). The comparison of INS 1 and INS 2 and the LAB runs reveals that such a boundary is indeed a transient depositional feature (Doppo and Stone 1994), related to flocculation within the water column and not easy to mimic in laboratory experiments. In a river experiment, Rhône River, France, it was shown that an observed fluff layer was mainly representative of recent deposits of originally suspended particles, probably trapped in the overlying water column during sediment sampling (El Ganaoui et al. 2004). Thus sampling and transporting sediments undisturbed from field to lab and then inserting them as cores into flumes poses a difficult experimental task. Average mass eroded in the LAB runs at same u^* was six times higher than that of the INS runs (Fig. 6.20), indicating a different degree of consolidation of the undisturbed Spree sediment. A new method of preparing flume cores has to be devised.

Table 6.8 indicates a homogenous particle distribution in the sediment layers experiencing resuspension since homogenization by the peristaltic pump was ruled out. However, the increasing dominance of heavier particles at an increasing u^* suggests a selective transport and the tendency of higher w_s as longer the sediment are exposed to higher u^* .

A high P entrainment arises at low u^* (Fig. 6.19, INS 1) from flocculated particles, initiating batch-wise P burdens and maintaining high percentages of particulate P in the flow (Fig. 6.23). In concordance with the increase of SPM concentration (Fig. 6.22) TP concentration can enhance temporarily. However, the resuspended, reprocessed or remoulded particles, such as detritus or feces, show significantly higher sinking velocities (Table 6.8) and masses than those from SPM (Fig. 6.22). These findings explain the large potential distances of particle and P transport known as 'P spiralling' varying between distances of 1 and 1000 m depending on w_s and the deposition stress (Gust and Kozerski 2000) of the sinking-particle distribution (e.g., Sharpley et al. 2003).

6.4.5 Conclusions

Laboratory microcosm experiments using sliced and pooled cores ensure a high reproducibility for particle cycling experiments, whereas in situ experiments describe the resuspension and deposition behaviors closer to reality. The latter require a larger sample size due to small-scale sediment heterogeneity. Low flow-generated shear velocities u^* can lead to batch-wise P burdens when resuspending freshly deposited materials of the fluff layer. Such events would be underestimated in laboratory experiments lacking this transient storage feature of rivers.

Acknowledgments

The authors are grateful to I. Henschke (BTU Cottbus) for technical assistance and scuba diving, to C. Herzog, A. Lüder, H.-J. Exner as well as M. Reiche (all IGB Berlin) for laboratory assistance, and D. Hoffmann and V. Müller (TUHH) for processing the particle images. This manuscript benefited from two anonymous reviewers. This study was financially supported by the Federal Ministry of Education and Research (BMBF, FKZ 02WF0469).

References

- Black KS, Tolhurst TJ, Paterson DM, Hagerthey SE (2002) Working with natural cohesive sediments. *Journal of Hydraulic Engineering* 128:2–8
- Bungartz H, Wanner SC (2004) Significance of particle interaction to the modelling of cohesive sediment transport in rivers. *Hydrological Processes* 18:1685–1702
- Droppo I, Stone M (1994) In-channel surficial fine-grained sediment laminae (part I): physical characteristics and formational processes. *Hydrological Processes* 8:101–111
- El Ganaoui O, Schaaff E, Boyer P, Amielh M, Anselmet F, Grenz C (2004) The deposition and erosion of cohesive sediments determined by a multi-class model. *Estuarine, Coastal and Shelf Science* 60:457–475
- Gust G (1990) Method of generating precisely-defined wall shear stresses. US Patent Number: 4,973,165/1990
- Gust G, Morris MM (1989) Erosion thresholds and entrainment rates of undisturbed in situ sediments. *Journal of Coastal Research* 5:87–99
- Gust G, Müller V (1997) Interfacial hydrodynamics and entrainment functions of currently used erosion devices. In: Burt N, Parker R, Watts J (eds) *Cohesive sediments*. Wiley, Chichester, UK, pp 149–174
- Gust G, Kozerski H-P (1997) In situ sinking particle flux from collection rates of cylindrical traps. *Marine Ecology Progress Series* 208:93–106
- Köhler J, Gelbrecht J, Pusch M (Hrsg.) (2002) *Die Spree – Zustand, Probleme, Entwicklungsmöglichkeiten*. *Limnologie Aktuell*, Bd. 10, E. Schweizerbart'sche Verlagsbuchhandlung, Stuttgart, pp 384
- Murphy J, Riley JP (1962) A modified single solution method for determination of phosphate in natural waters. *Analytica Chimica Acta* 27:31–36
- Redondo JM, Durrieu de Madron X, Medina P, Sanchez MA, Schaaff E (2001) Comparison of sediment resuspension experiments in sheared and zero-mean turbulent flows. *Continental Shelf Research* 21:2095–2103
- Shand CA, Smith S, Edwards AC, Fraser AR (2000) Distribution of phosphorus in particulate, colloidal and molecular-sized fractions of soil solution. *Water Research* 34(4):1278–1284
- Sharpley A, Krogstad T, McDowell R, Kleinman P (2003) Phosphorus transport in riverine systems. *Encyclopedia of Water Science*, Marcel Dekker Inc. New York
- Svendsen LM, Kronvang B, Kristensen P, Graesbol P (1995) Dynamics of phosphorus-compounds in a lowland river system – importance of retention and nonpoint sources. *Hydrological Processes* 9(2):119–142
- Tengberg A, Stahl H, Gust G, Müller V, Arning U, Andersson H, Hall POJ (2004) Intercalibration of benthic flux chambers I. Accuracy of flux measurements and influence of chamber hydrodynamics. *Progress in Oceanography* 60:1–28
- Thomas SA, Newbold JD, Monaghan MT, Minshall GW, Georgian T, Cushing CE (2001) The influence of particle size on seston deposition in streams. *Limnology and Oceanography* 46(6):1415–1424
- Witt O, Westrich B (2003) Quantification of erosion rates for undisturbed contaminated cohesive sediment cores by image analysis. *Hydrobiologia* 494:271–276

6.5 Determination of Heavy Metal Mobility from Resuspended Sediments Using Simulated Natural Experimental Conditions

6.5.1 Introduction

Heavy metal loads in river flows continue to decrease due to better control and pre-treatment of wastewater. However metal release still occurs, e.g., from abandoned mining sites, diffuse input, and contaminated floodplains. Metals discharged into aquatic systems are mostly adsorbed on suspended particles and fine grained riverine sediments which are predominantly deposited in groyne fields and harbor basins. Distribution, mobility and bioavailability of heavy metals in rivers do not simply depend on total concentrations but, critically, on their chemical and physical associations and on transformation processes they undergo. Gradually, contaminant potentials are formed in the sediments, from which under changing chemical conditions heavy metals can be mobilized (Hong et al. 1991; Peiffer 1997). Understanding possible mobilization and transformation effects of metals bound to sediments requires detailed studies of release mechanisms and how they are affected by hydrodynamic and biogeochemical processes (Calmano et al. 2005).

Anoxic sediment deposits are the main source for a secondary release and the spread of contaminants (Förstner et al. 1999). The main reason for reduction processes in limnic and marine sediments is the degradation and mineralization of organic substances through microbial activity. Oxygen consumption in an anaerobic environment results in formation of metal sulfides and/or carbonates. These minerals are stable in the sediments until oxygen becomes available, e.g., by dredging, flood events or tidal streams. These disturbances are followed by several simultaneous processes: desorption, diffusion of contaminants into the water phase from pore waters, mineral dissolution processes, relocation of sediment-bound contaminants, and oxidation processes. Oxidation of sulfides produces sulfuric acid which may lower the pH in micro zones of the sediment, dissolve other mineral phases, e.g., carbonates, and can lead to the further release of heavy metal ions (Calmano et al. 2005). A summary of the main factors is shown in Fig. 6.24.

Criteria for the prognosis of the middle- and long-term behavior of metals in sediments should include the acid production capacity (APC) of the system as well as abilities for neutralizing acidic constituents. In a sediment/water system, the most important reactions producing hydrogen ions are oxidation of inorganic and organic sulfur-, nitrogen- and iron-species (Hong et al. 1994). The buffering or acid neutralizing capacity (ANC) may be attributed to the acid neutralization capacity of the solids and that of the dissolved phase.

Most river sediments are well buffered against acidification, as can be shown by acid titrations. Dissolution of carbonates occurs at neutral to slightly acidic pH, ion exchange capacities of clay minerals maximize at pH 5, dissolution of aluminum hydroxides begins at pH 4, and the dissolution of iron hydroxides at pH 2. Under certain conditions mobilization and transfer of sediment bound heavy metals may also occur at neutral pH, e.g., at changes of the ion concentration (displacement by ion exchange and/or complexation) or by microbial reactions (methylation).

Dissolved metal concentrations are not only controlled by release reactions but also by re-adsorption processes on suspended material. In a multi-chamber system the metal

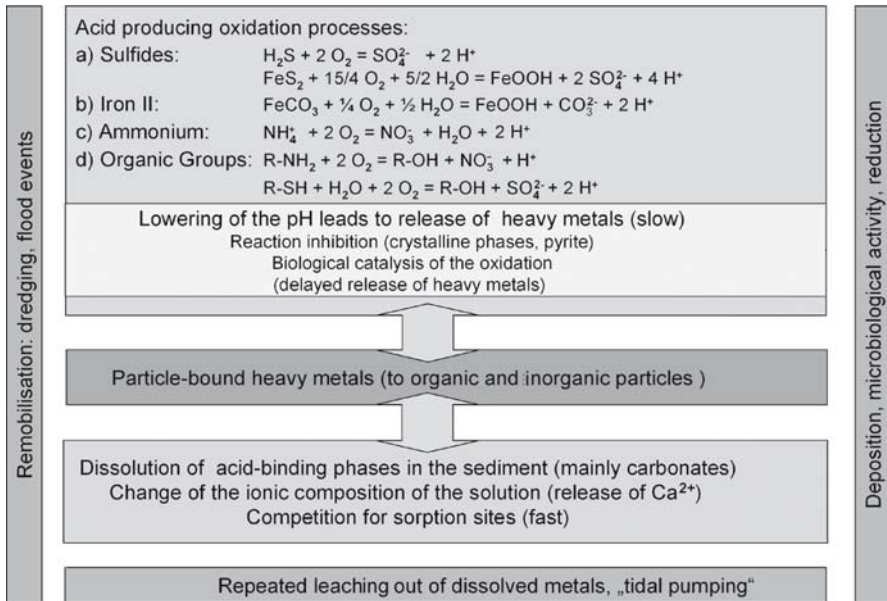


Fig. 6.24. Overview of chemical processes that follow sediment resuspension until the sediment is re-deposited

transfers from anoxic sediments to competitive re-adsorption sites on different sediment model compounds were studied during oxidation experiments (Calmano et al. 1988). These studies showed that e.g., the transfer of copper to quartz sand and clay was negligible, a small fraction was transferred to Mn- and Fe-oxides, and the main fraction could be found adsorbed to algal cell walls representing the organic part of the sediment.

Calculation of the solubility of heavy metals in reduced sulfidic sediments indicates supersaturation for most metals, but they were nevertheless available to thin film gradient (DGT) measurement (Naylor et al. 2004, 2006). This suggests that even under anoxic conditions, there is a dynamic pseudo-steady state where metals are not bound as sulfides in an inert, insoluble phase, but are released into the pore water and re-adsorbed onto suspended matter. In the in situ perturbation experiment from Naylor et al. the pore-water equilibrium was disturbed by inducing a flux from the pore water to the probe, showing the dynamic response of sediments in the transfer of metals.

6.5.2 Experiments

Sediment Composition

Sediment samples were taken from different locations at the river Elbe, upstream of the Hamburg Harbor, and in the channels of the Hamburg Harbor. The sampling sites are shown in Fig. 6.25.

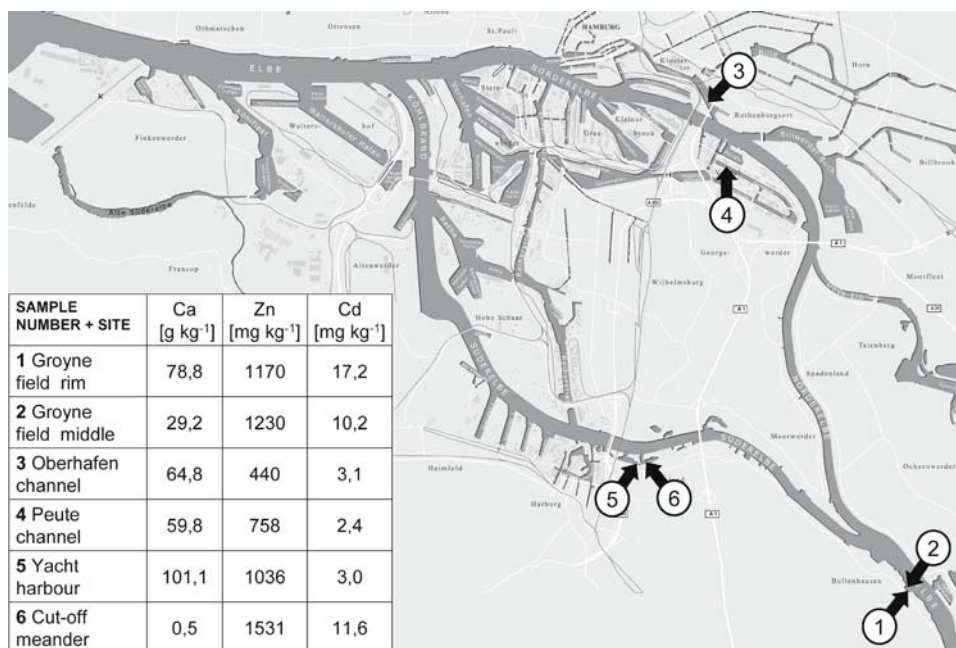


Fig. 6.25. Overview of the different sampling sites at the river Elbe and in the Hamburg Harbor and some selected metal contents of the sites. (1, 2) Groyne field at Elbe-km 607.7 that was sampled monthly by several workgroups of the SEDYMO Project. (3) “Oberhafenkanal”, harbor channel close to the Norderelbe. (4) “Peutekanal”, harbor channel in Veddel. (5) Yacht Harbor at the Süderelbe. (6) “Schweenssand”, a cut-off meander at the Süderelbe

The sediments showed very different calcium contents ranging from 0.5% (site 6) to 10% (site 5). Most of the sediments are rather rich in calcium. As there are no major sources of calcite in the catchment area, the Elbe sediments were expected to be poor in calcium. The high contents, therefore, can only be explained by biogenic decalcification of the supernatant waters. X-ray diffraction analyses of the upper 6 cm of an Elbe River sediment core demonstrated calcite and quartz as the main constituents (Schwartz 2006).

Metal contents were high in the groyne field (sites 1 and 2), but showed slight variations due to different sampling locations. The measured values in the harbor channels (sites 3 and 4) were approximately half of the contents directly at the river for all metals.

Sediment Depth Profiles

The sediment used for the experiments described below was retrieved from the sampling site “Schweenssand” (6). It is connected to the main stream that supplies frequent tidal flooding of the area with short intermediate dry periods. A sediment core was taken at the sampling site for the later resuspension experiments and cut into cm-layers to obtain a depth profile of the metal contents of the complete sediment (Fig. 6.26). Dry sieving of the sediment slices resulted in 3 grain size fractions: Small slug shells

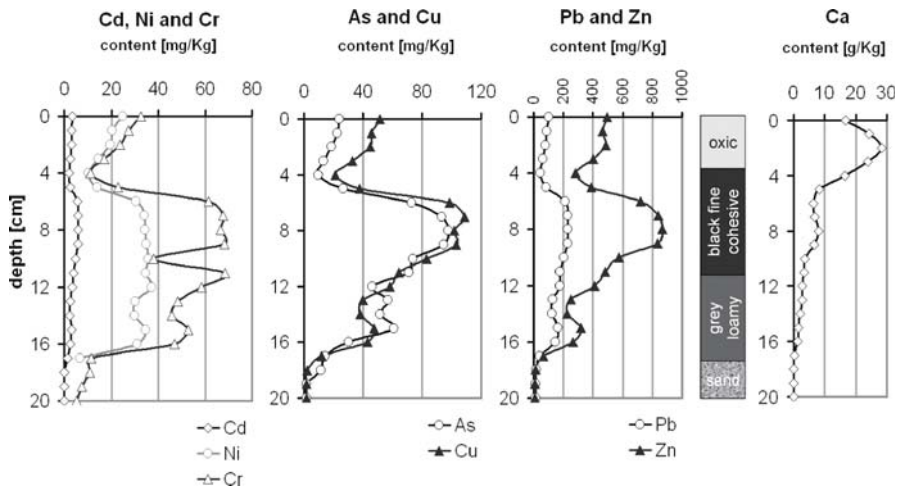


Fig. 6.26. Depth profile of metal contents at the sampling site for resuspension experiments. The metal contents were measured without separating grain size fractions

above 1 mm, quartz sand from 1 mm to 0.063 mm, and the cohesive fine fraction smaller than 0.063 mm. Metal contents were much higher in the fine-grained anoxic zone of the sediment (see 4–12 cm), whereas Ca-concentrations were highest close to the sediment surface.

Experimental Setup for the Resuspension Experiments

To study both short- and long-term processes during sediment resuspension and to simulate erosion by a flooding event we took an undisturbed groyne field sediment core from sampling site (6) and transferred it directly from the field into an erosion apparatus or “water column simulator”, that was developed and supplied by the Institute of Marine Engineering at Hamburg University of Technology (see Müller et al. this volume). The sample was taken in December at winter conditions. The water temperature was 6 °C, so the phytobenthic activity was very weak. Freshly collected river water was used as a supernatant. The chloride concentration of the supernatant water was 150 mg l⁻¹. The apparatus, equipped with an adjustable stirring unit was placed in a climatic chamber at a constant temperature of 12 °C in the dark to prevent phytobiotic activity (Fig. 6.27).

After a consolidation phase of 2 weeks, the upper, mainly oxic layer of the sediment was eroded and kept in suspension above the remaining sediment core.

The apparatus was open to allow diffusion of oxygen during the experiment.

After 27 days, the total supernatant suspension was removed and transferred to a separate vessel where it was kept in suspension by continuous stirring and monitoring. Following this, fresh river water was refilled to simulate the water change that normally occurs frequently, and a further part of the remaining anoxic core layer was resuspended to simulate another erosion event without the presence of the upper oxic sediment layer. This part of the experiment lasted for 14 days.

Fig. 6.27. “Water column simulator” with inserted DGT devices before start of the resuspension, and during resuspension of the anoxic layer. The inner diameter of this device is 29 cm and the used height is 59 cm



With the use of the “water column simulator” as an erosion device for natural sediment, a linking of hydrodynamic and chemical factors was possible. The critical shear force of erosion for both the oxic and anoxic layer was determined. The suspended mass was quantified and analyzed, as well as the solute composition. Monitoring of metal release during erosion provided the amount of metals bound to suspended particles, the amount of metals dissolved in solution, and by the use of thin film gradient technique (DGT) the dissolved amount that might be readily bioavailable.

The samples were taken in the upper part of the “water column simulator”, so that only the fine fraction of the resuspended sediments was measured. During the experiment eroded sand grains or those released from the breakdown of the suspended agglomerates resettled quickly and therefore were not sampled.

6.5.3 Results

Controlled Resuspension of the Oxic Sediment Layer

Critical shear velocity for the initial erosion of 3.4 cm of the oxic sediment layer within 12 hours was $u^* = 2.23 \text{ cm s}^{-1}$. This shear velocity was kept constant during the first phase of the erosion (27 days). The metal content of the resuspended sediment from the oxic layer (Table 6.9) were much higher than the bulk concentrations found in the corresponding layers of the sediment core. This is due to the higher fine grain content of the sediment suspension at the top of the stirred column.

The redox potential of the solution as well as oxygen saturation and pH (6.7) remained constant throughout the experiment. Nevertheless, we observed an increase in sulfate concentration in solution, as well as a decrease of hydrogen carbonate (see

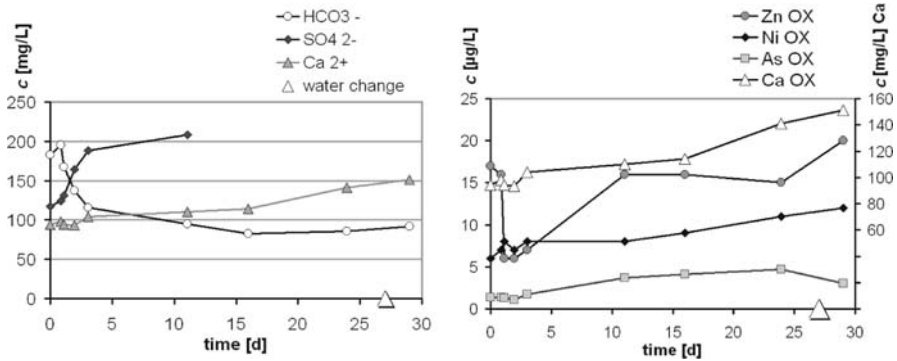


Fig. 6.28. Sulfate, hydrogen carbonate, calcium and metal contents of 0.2 μm -filtrates obtained during the oxic layer resuspension

Fig. 6.28), which indicates the presence of reduced sulfur compounds close below the oxidic sediment water interface. These processes occur quickly in the first three days of erosion. Obviously the initial small amount of acidity produced is neutralized by the water alkalinity, since no release of Ca was observed during the first three days. Further slow oxidation supplies more H^+ indicated by the dissolution of carbonates and the release of Ca, as noted after day 3.

The Ni and As concentrations in the supernatant solution did not increase during the actual oxidation phase (first three days), then increased slowly (see Fig. 6.28). This release is correlated to the carbonate dissolution process. Zn present in solution at the beginning of the experiment was partially adsorbed on the suspended particles and removed from the solution. However, Zn concentration in solution increased again after 5 days. We suppose that Zn is released either from the dissolution of mineral phases during the experiment, or from the breakdown of aggregates during the prolonged stirring process.

Controlled Resuspension of the Anoxic Sediment Layer

Critical shear velocity for the secondary erosion of 4.8 cm of anoxic sediment layer within 12 hours was $u^* = 2.80 \text{ cm s}^{-1}$, indicating a strongly compacted older sediment layer. Here, the redox value of the solution as well as the oxygen content dropped immediately after the start of the suspension from an initial value of 220 mV to 20 mV, but recovered within a day and slowly approached the initial values within 4 days. Oxidation of metal sulfides is indicated by a strong release of sulfate, whose formed acid consumed part of the hydrogen-carbonate buffer and lead to a simultaneous release of Ca. The pH value did not change. These reactions naturally terminated after day 4 (see Fig. 6.29).

Ca and Ni measured in solution, with the given detection limits of the analytical instruments, showed a steep increase in concentration following the oxidation reaction, whereas Zn was removed from the solution during the first phase of the oxidation reaction, as shown in Fig. 6.29. After 24 hours more Zn is released than was measured in the initial solution concentration. This supports the suggestion of a secondary Zn release by dissolution of mineral phases and breakdown of aggregates during the stirring process. Arsenic was released from the pore water.

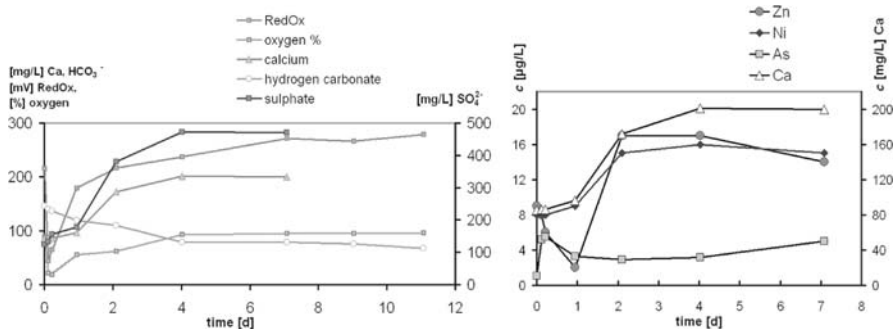
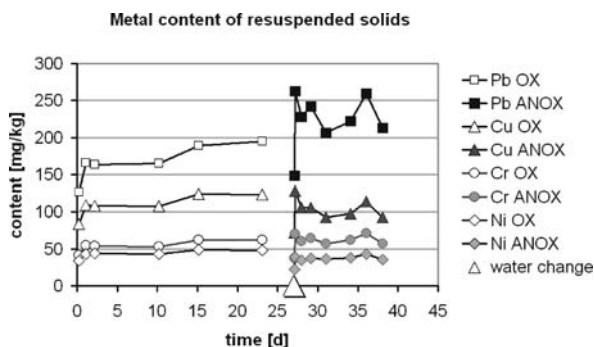


Fig. 6.29. Redox potential, oxygen content and significant ion concentrations during resuspension of the anoxic layer. The *right graph* shows the metal contents of 0.2-µm filtrates

Fig. 6.30. Metal contents of the particles filtered during oxic and anoxic layer resuspension



Resuspension of Particle Bound Metals

Resuspension of the *oxic* layer yielded a concentration of 20 g l⁻¹ solids at the top of the column measured by filtration. During resuspension of the *anoxic* layer, 30 g l⁻¹ solids were suspended. While the core analysis showed lower metal contents in the oxic layer, the metal contents of the suspended sediments were nearly equal in both resuspension experiments, as shown in Fig. 6.30. This can be explained by a grain size fractionation: Only the strongly-contaminated fine fraction of the sediment is retrieved at the top of the suspension chamber.

Table 6.9 summarizes the amount of resuspended solids and their metal contents. Compared to the dissolved concentrations, the particle-bound amount was a factor of 1 000 larger than the amount in solution for Zn, and still a factor of 100 larger for Ni.

DGT Measurements

In a “differential gradient in thin films” (DGT) probe an array of polyacrylamide hydrogel with a layer of Chelex 100 ion exchange resin, a diffusion gel layer of defined thickness and a filter membrane cover is held in a rigid plastic housing that provides a defined exposure area. Dissolved metal compounds and those bound in small complexes can diffuse through the filter and gel layer and are adsorbed completely at the

Table 6.9. Solid concentrations and concentration of metals bound to suspended material

	Solids (g l ⁻¹)	Zn (mg l ⁻¹)	Pb (mg l ⁻¹)	Cu (mg l ⁻¹)	Cr (mg l ⁻¹)	Ni (mg l ⁻¹)	Cd (mg l ⁻¹)
Oxic layer	20	22	3	2	1	0.8	0.16
Anoxic layer	30	40	7	3	2	1.2	0.20

resin layer, where hence the solution concentration is zero. This results in a linear concentration gradient through the diffusive layer. The mass of metal accumulated in the resin is obtained by leaching the Chelex gel with acid and analyzing the leachate. With the given immersion time of the gel, the exposure area, the thickness of the diffusion layer and the diffusion coefficient for each metal in the layer the time-average solution concentration of not or only weakly bound metal species can be calculated (Davison and Zhang 1994).

DGT can be used to determine the “bioavailable” fraction of metals, since it is assumed that only free dissolved metal ions and those released from labile complexes pass through the diffusion layer (Tusseu-Vuillemin et al. 2003). Newer studies show that meta-stable organic complexes can also be determined with DGT, so that the results have to be interpreted with caution concerning predictions about bioavailability (Buzier et al. 2006).

The thin film gradient devices were immersed in the suspension for specific time spans, mostly 4 days. While only Zn, Ni and As concentrations in the suspension filtrates exceeded the detection limits of the analytical instruments, more metals could be detected by the accumulation in DGT devices.

Part of the metals is bound in stable complexes and colloidal particles that pass the filter but are not detected by the DGT devices, so the concentrations measured with the DGT method were only 25 to 50% of those determined in the 0.2- μ m filtrates.

The DGT-measured metal species showed different behavior (see Fig. 6.31). Zn follows the solution concentration, whereas the amount of Ni remained constant even though the solution concentration is doubled in the anoxic suspension.

Cu concentrations increased slowly during the experiment, but more Cu was released during resuspension of the oxic layer. An increase could also be measured in solution after day 11.

Cd showed a similar release behavior as Zn, but without the initial re-adsorption from solution. This strengthens the suggestion that the release process of Zn is slow due to mineral dissolution by oxidation or de-agglomeration.

6.5.4 Discussion and Conclusions

Erosion of the oxic and anoxic layer of the studied Elbe River sediment needed shear velocities of $u^* = 2.20\text{--}2.80 \text{ cm s}^{-1}$. These values were rather high compared to other, non-cohesive inland river sediments normally ranging from $u^* = 0.3\text{--}1.8 \text{ cm s}^{-1}$ (Gust, pers. comm.). It can be assumed that these compacted groyne field sediments can only be mobilized by dredging operations.

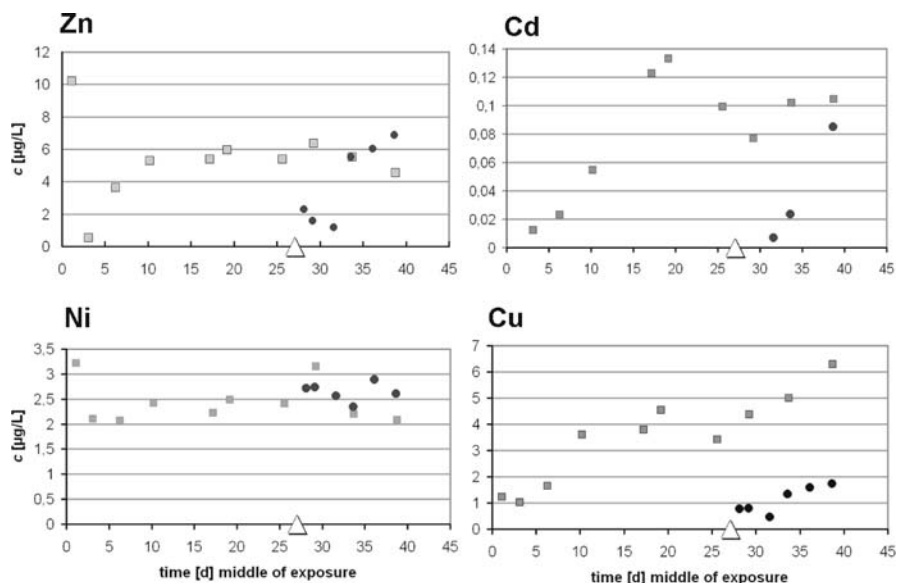


Fig. 6.31. Accumulated metal concentrations during 4 days measured with thin film gradient technique (DGT). The *square light gray dots* represent the values of the oxic layer resuspension, the *round dark dots* show the values of the anoxic layer resuspension

During resuspension in the “water column simulator” particle aggregates are broken down and a separation of grain sizes arises in the column. The gradient of grain sizes favors the short-term resettling of coarser sand particles and long-term suspension of the highly contaminated fine fraction of the sediment (“washing effect”).

During the whole experiment the buffer capacity of the sediment was not exceeded and the pH remained constant at 6.7. The release of SO_4^{2-} , and the consumption of HCO_3^- indicates acid formation from sulfides during the resuspension of the oxic layer.

Remobilization of heavy metals was affected by different effects. In both resuspension experiments about 70% of the initially dissolved Zn was immediately adsorbed on the resuspended sediment particles. During the first day of resuspension of the oxic layer increase of sulfate concentration indicates the release of acidity, but no rise in the concentration of dissolved metals was found. Later a very slow increase of Zn and Ni concentrations were observed in solution. This may be due to the breakdown of aggregates, following weak oxidation processes and dissolution of some metal compounds. Ca was also released slowly but the carbonate buffer of the sediment was barely influenced by the initial minor acid production.

During resuspension of the anoxic layer Zn and Ni were mobilized parallel to the production of sulfate and the release of Ca until day 4. While in the case of oxic sediment the release of metals is slow, in anoxic sediment it is fast and enhanced by the effects discussed above.

Even at pH-neutral conditions resuspension of the anoxic layer leads to a minor release of Zn and Ni during the actual oxidation. While the total dissolved concentrations, determined in the 0.2- μm filtrates, were higher during resuspension of the *an-*

oxic sediment layer, the amount of free hexaquo ions and labile complexes measured by DGT were in the same range for *both* cases, and for Cu they were only 1/10 of the oxic case.

The results of this study indicate that even at shear velocities that affect only the oxic layer of sediment and may be caused by tidal movements of the water body in river estuaries, small amounts of free Zn, Cd and Cu ions are released into the water body. These release processes are not due to the initial resuspension process, but develop in a time span of more than a week. It can be assumed that this slow release is mediated by the breakdown of aggregates, desorption and dissolution of incorporated metal compounds.

This results can be seen as a link to further delayed release processes (Fengler et al. 1999). In case of resuspension of anoxic sediment layers, the release process of heavy metals is governed by the initial oxidation process. Although no pH change could be measured, more acid is produced, followed by ion exchange processes at the sediment matrix. The oxidation of sulfides to sulfate happens rather fast, the main part is oxidized within two days. The metals release is low, because there is no change in the pH during the process. The complete release of heavy metals from suspended sediments can be summarized in three steps: (1) Immediate release from oxidation and matrix exchange processes. (2) Mid-term release from the oxidized resuspension, probably caused the physical breakdown of agglomerates. (3) Delayed long-term release by acidification if no sufficient buffer capacity is available (Fengler et al. 1999).

Although the first two processes only lead to very low dissolved concentrations of heavy metals, compared to the amount bound on resuspended sediment particles, a repeated leaching of sediments that undergo frequent suspension-deposition-cycles, such as the upper oxic layers of harbor basin sediments, may contribute significantly to the heavy metal load released and spread in the water body.

Acknowledgments

We would like to thank Prof. G. Gust (Hamburg University of Technology) and his co-workers for fast technical support during the experiments, Dr. G. Fengler (University of Greifswald) and A. Matthäi (Hamburg University of Technology) for sampling and additional analysis, and the German Federal Ministry of Education and Research for financial support.

References

- Buzier R, Tusseau-Vuillemin M-H, Mouchel J-M (2006) Evaluation of DGT as a metal speciation tool in wastewater. *Sci Tot Environ* 358:277–285
- Calmano W, Ahlf W, Förstner U (1988) Study of metal sorption/desorption processes on competing sediment components with a multichamber device. *Environ Geol Water Sci* 11:77–84
- Calmano W, von der Kammer F, Schwartz R (2005) Characterization of redox conditions in soils and sediments: heavy metals. In: Lens P, Grotenhuis T, Malina G, Tabak H (eds) *Soil and Sediment remediation*, IWA Publ. London UK, pp 102–120
- Davison W, Zhang H (1994) In situ speciation measurements of trace components in natural waters using thin-films gels. *Nature* 367:546–548

- Fengler G, Förstner U, Gust G (1999) Verification experiments on delayed metal release from sediments using a hydrodynamically controlled erosion apparatus (in German). Abstract Annual Meeting German Society of Water Chemistry, Regensburg, pp 240–243
- Förstner U, Calmano W, Ahlf W (1999) Sedimente als Schadstoffsenken und -quellen: Gedächtnis, Schutzgut, Zeitbombe, Endlager. In: Frimmel FH (Hrsg.) Wasser und Gewässer – Ein Handbuch, Spektrum Akademischer Verlag Heidelberg, pp 249–279
- Hong J, Calmano W, Wallmann K, Petersen W, Schroeder F, Knauth H-D, Förstner U (1991) Change in pH and release of heavy metals in the polluted sediments of Hamburg-Harburg and the downstream Elbe during oxidation. In: Farmer JG (ed) Heavy Metals in the Environment, vol. 2. CEP Consultants, Edinburgh, pp 330–333
- Hong J, Förstner U, Calmano W (1994) Effects of redox processes on acid-producing potential and metal-mobility in sediments. In: Hamelink JL, Landrum PF, Bergman HL, Benson WH (eds) Bioavailability – Physical, Chemical and Biological Interactions, Lewis Publishers, Boca Raton, pp 119–141
- Naylor C, Davison W, Motelica-Heino M, Van Den Berg GA, Van Der Heijdt LM (2004) Simultaneous release of sulfide with Fe, Mn, Ni and Zn in marine harbour sediment measured using a combined metal/sulfide DGT probe. *Sci Tot Environ* 328:275–286
- Naylor C, Davison W, Motelica-Heino M, Van Den Berg GA, Van Der Heijdt LM (2006) Potential kinetic availability of metals in sulphidic freshwater sediments. *Sci. Tot. Environ.* 357:208–220
- Peiffer S (1997) Umweltgeochemische Bedeutung der Bildung und Oxidation von Pyrit in Gewässer-sedimenten. Bayreuther Forum Ökologie, Universität Bayreuth, vol. 47
- Schwartz R (2006) Geochemical characterization and erosion stability of fine-grained groyne field sediments in the Middle Elbe River. *Acta Hydrochim Hydrobiol* 34:223–233
- Tusseau-Vuillemin M-H, Gilbin R, Taillefert M (2003) A dynamic numerical model to characterize labile metal complexes collected with diffusion gradient thin films devices. *Environ Sci Technol* 37:1645–1652